2-Benzylpiperazine: a new scaffold for potent human Carbonic Anhydrase inhibitors. Synthesis, enzyme inhibition,

2-Benzylpiperazine: a new scaffold for potent human Carbonic Anhydrase inhibitors. Synthesis, enzyme inhibition, enantioselectivity, computational and crystallographic studies and in vivo activity for a new class of intraocular pressure lowering agents.

Niccolò Chiaramonte,[a] Silvia Bua,[a] Marta Ferraroni,[b] Alessio Nocentini,[a,c] Alessandro Bonardi,[a,c] Gianluca Bartolucci,[a] Mariaconcetta Durante,[d] Laura Lucarini,[d] Donata Chiapponi,[b] Silvia Dei,[a] Dina Manetti,[a] Elisabetta Teodori,[a] Paola Gratteri,[a,c] Emanuela Masini,[d] Claudiu T. Supuran,[a]* Maria Novella Romanelli[a]*

[a] University of Florence, Department of Neuroscience, Psychology, Drug Research and Child's Health, Section of Pharmaceutical and Nutraceutical Sciences, Via Ugo Schiff 6, 50019, Sesto Fiorentino (Italy)

[b] University of Florence, Department of Chemistry, via della Lastruccia, 50019 Sesto Fiorentino (Italy)

[c] University of Florence, Department NEUROFARBA – Pharmaceutical and Nutraceutical section; Laboratory of Molecular Modeling Cheminformatics & QSAR, University of Firenze, via Ugo Schiff 6, I-50019 Sesto Fiorentino, Firenze, Italy

[d] University of Florence, Department of Neuroscience, Psychology, Drug Research and Child's Health, Section of Pharmacology and Toxicology, Viale Gaetano Pieraccini 6, 50100 Florence (Italy)

* phone 0039 055 4573691 e-mail: novella.romanelli@unifi.it

* phone 0039 055 4573729 e-mail: claudiu.supuran@unifi.it

Key words carbonic anhydrase; enzyme inhibitors; piperazine; enantioselectivity; glaucoma.

Abstract

Two series of 2-benzylpiperazines have been prepared and tested for the inhibition of physiologically relevant isoforms of human carbonic anhydrases (hCA, EC 4.2.1.1). The new compounds carry on one nitrogen atom of the piperazine ring a sulfamoylbenzamide group as zinc-binding moiety, and different alkyl/acyl/sulfonyl groups on the other nitrogen. Regio- and stero-isomers are described. The majority of these compounds showed Ki values in the low-medium nanomolar range against hCA I, II and IV, but not IX. In many instances interaction with the enzyme was enantioselective. The binding mode has been studied by means of X-ray crystallography and molecular modelling. Two compounds, evaluated in rabbit models of glaucoma, were able to significantly reduce intraocular pressure, making them interesting candidates for further studies.

Introduction

Carbonic Anhydrase (CA, EC 4.2.1.1) is a very efficient enzyme, which catalyzes the hydration of carbon dioxide to produce bicarbonate and a proton. This process is crucial for most organisms, and, as a consequence, during the evolution of life seven genetically different families of this enzyme (classified as α- θ-CAs) evolved [1]. α-CA are present in vertebrate, and in mammals 16 different α-CA isoforms were isolated and characterized so far, varying for tissue distribution and cellular localization (membrane, cytosol, mitochondria) [2]. Some isoforms have been studied in detail also by means of X-ray crystallography, obtaining pictures of the active site, where a zinc ion plays a pivotal role in the catalytic reaction. Moreover, other structural features of the active site have been highlighted, such as the presence of two different areas, one lined by hydrophobic residues and the other one by hydrophilic aminoacids, offering the opportunity to modulate ligand design in different ways [3].

CA inhibitors are in clinical use for more than sixty years as diuretics and antiglaucoma drugs [4]. Glaucoma is a multifactorial ocular disease characterized by optic nerve degeneration generally related to high intraocular pressure, which can lead to blindness [5]. CA inhibitors such as dorzolamide and brinzolamide are effective in reducing intra-ocular pressure (IOP) after topical administration; however, since these drugs display several side effect, novel therapeutic agents are needed [6]. The isoform mainly involved in aqueous humor secretion are CA II and CA IV [7]. Oral and topical CA inhibitors are also used in other ocular diseases, among which cystoid macular oedema [8].

Classical inhibitors contain a benzene or heterocyclic sulfonamide moiety, which coordinates the zinc ion. This pharmacophoric group has been inserted into a variety of structures obtaining compounds endowed with high potency and in some instances isoform selectivity [3]. Due to the high number of CA isoforms, potency and selectivity are crucial properties for therapeutic applications, especially those suggested in recent times, such as anticonvulsant, antiobesity, anticancer, analgesic, and antiinfective drugs [9-13].

The piperazine ring is a widely used scaffold for drug discovery, and piperazine derivatives are known to produce a wide range of pharmacological activities [14]. Several piperazines have been tested also on CA, showing a broad spectrum of potency; some examples are shown in Chart 1. Compounds **I** and **II** are mainly N-arylpiperazines, carrying an arylsulfonamide moiety as zinc binding group (ZBG), linked to the second piperazine N-atom directly (**II**) or through an urea moiety (**I**). Both series of molecules were tested on hCA I, II, IX and XII. Compounds with general formula **I** showed good potency (K_i in the low nanomolar) especially on hCA II, and in few instances also on hCA IX (Ar = phenyl or 4-Cl-phenyl) or hCA XII (Ar = 3-cyano-2-pyridinyl, 4-trifluoromethyl-2-pyrimidinyl) [15]. Compounds with general formula **II** were weaker inhibitors (K_i in the high nanomolar), the less sensitive enzyme being hCA I; only few compounds showed K_i values below 50 nM on hCA XII (R = benzyl, 2-pyrimidinyl) or on hCA IX (R = benzyl) [16]. Other examples of piperazine-based CA inhibitors can be found in the literature [17, 18], but to our knowledge, no C-substituted piperazine has been tested so far on hCA.

Chart 1

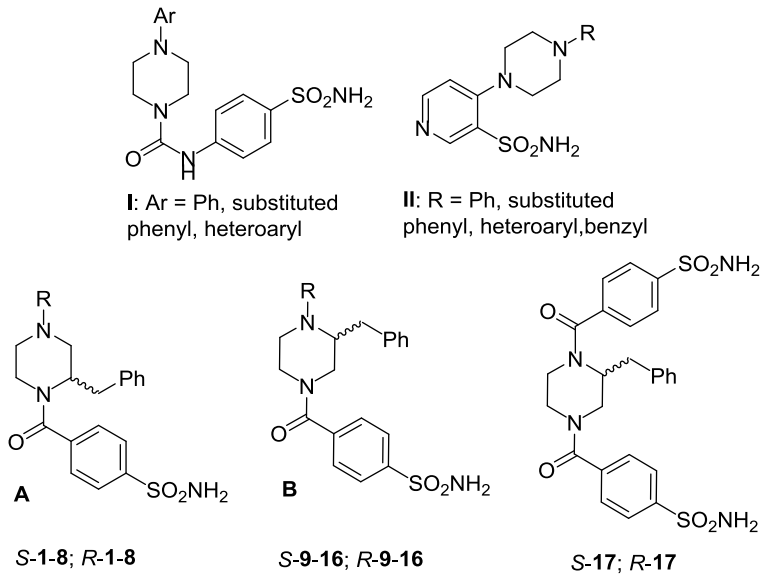

I: Ar = Ph, substituted phenyl, heteroaryl

II: R = Ph, substituted phenyl, heteroaryl,benzyl

A

S-**1**-**8**; *R*-**1**-**8**

B

S-**9**-**16**; *R*-**9**-**16**

S-**17**; *R*-**17**

Aiming to find new potent and selective CA inhibitors, we designed and prepared two series of compounds (A and B), characterized by the presence of a piperazine ring carrying a

sulfamoylbenzamide moiety as ZBG on one N atom, and different alkyl/acyl/sulfonyl groups on the other one. The 6-membered ring has been further decorated with a lipophilic substituent (e.g. a benzyl group), which could interact with the lipophilic area of the active site, while the amide linkers or the chargeable amine functionality could be engaged with the hydrophilic domain. In our design these interactions could introduce high potency and hopefully also some isoform selectivity. Thus, compounds **1**-**16** were prepared and tested as CA inhibitors on four different isoforms (hCA I, hCA II, hCA IV and hCA IX), together with the serendipitously discovered **17**, which could comply with both A and B general formulas. The presence in these molecules of a stereogenic centre prompted us to synthesize both the *R* and *S* enantiomers, allowing us to perform a study of enantioselectivity, in order to understand the features associated with effective enzyme inhibitory properties.

Chemistry

Compounds reported here were synthesized following the procedures shown in Schemes 1-3. The enantiomers were prepared starting from the suitable (*S*) or (*R*) synthone using the same methods, with the exception of compounds (*S*)-**11** and (*R*)-**11**, which were prepared in different ways.

The synthesis of compounds with general formula A started from (*S*) or (*R*)-1,3 dibenzylpiperazine **18** (Scheme 1), obtained as reported by Gerdes [19]. Treatment of (*S*) or (*R*)-**18** with 4-sulfamoylbenzoyl chloride in acetonitrile gave amides (*S*) and (*R*)-**1** which underwent catalytic hydrogenation, leading to secondary amines (*S*)- and (*R*)-**2**. Compounds (*S*) and (*R*)-**3**-**8** were then obtained treating **2** with the suitable reagent in acetonitrile. Triethylamine was added when this reaction was performed with acid chlorides (benzoyl chloride for **5**, methanesulfonyl chloride for **7**, phenylsulfonyl chloride for **8**). The base was not necessary when preparing compounds **4** and **6**, for which acetic anhydride or 2,5-dioxopyrrolidin-1-yl 2-phenylacetate [20],

respectively, were used, nor for the synthesis of **3**, for which only 0.5 eq of methyl iodide were used.

Scheme 1

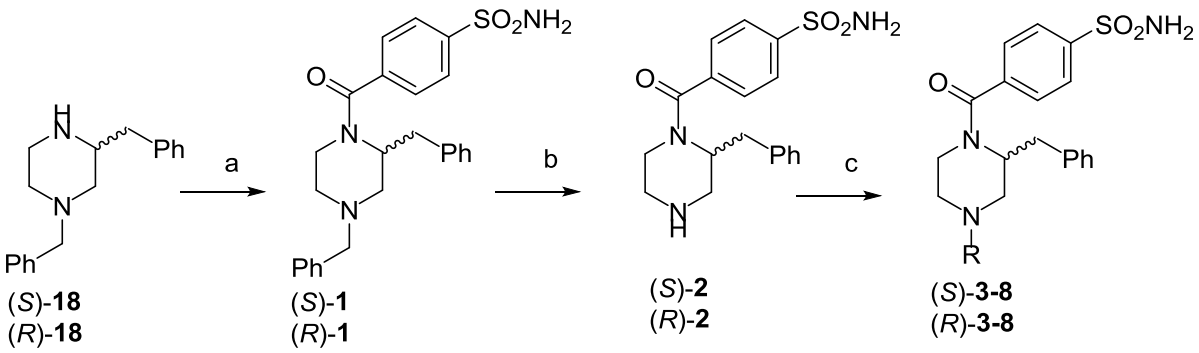

Reagents: (a) 4-sulfamoylbenzoyl chloride, TEA, acetonitrile; (b) MeOH/HCl, H_2/Pd/C; (c) R-Z, acetonitrile, base (when necessary). For the meaning of R-Z and base see Table 3.

(*S*)-**18** was used also in the synthesis of (*S*)-**11** (Scheme 2). It was treated with formic acid/formaldehyde to give the *N*-methyl derivative (*S*)-**19**, then its catalytic hydrogenation led to the secondary amine (*S*)-**20** [21]. Reaction with 4-sulfamoylbenzoyl chloride gave the desired *N*-methyl derivative (*S*)-**11.**

Scheme 2

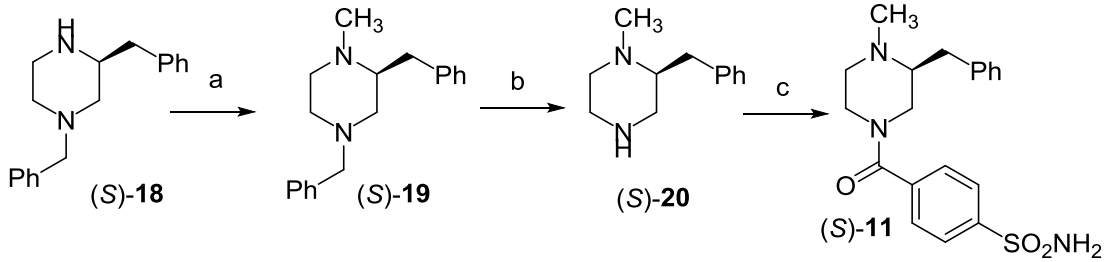

Reagents: (a) formaldehyde, formic acid, abs EtOH; (b) MeOH/HCl, H_2/Pd/C; (c) 4-sulfamoylbenzoyl chloride, TEA, acetonitrile.

The synthesis of the other compounds with the general formula B started from (*S*) or (*R*)-2-benzyl piperazine **21** (Scheme 3), obtained as reported by Levy [22]. Treatment of (*S*) and (*R*)-**21** with 4-sulfamoylbenzoyl chloride at room temperature afforded almost exclusively the double addition products (*S*) and (*R*)-**17**. (*S*) and (*R*)-**9** were obtained by reaction of (*S*) and (*R*)-**21** at 0°C with 0.7 eq of 2,5-dioxopyrrolidin-1-yl 4-sulfamoylbenzoate [23], in order to avoid the formation of

the double addition product **17** [24], and transformed into the final compounds (*S*) or (*R*)-**12**-**16** as done for their regio-isomers (compounds **4**-**8** A series). The N-benzyl derivatives (*S*) and (*R*)-**10** were obtained by reaction of (S) or (R)-**9** with benzyl bromide using $NaHCO_3$ as base, while for compound (*R*)-**11** methyl iodide (0.5 eq) was used without addition of a base.

Scheme 3

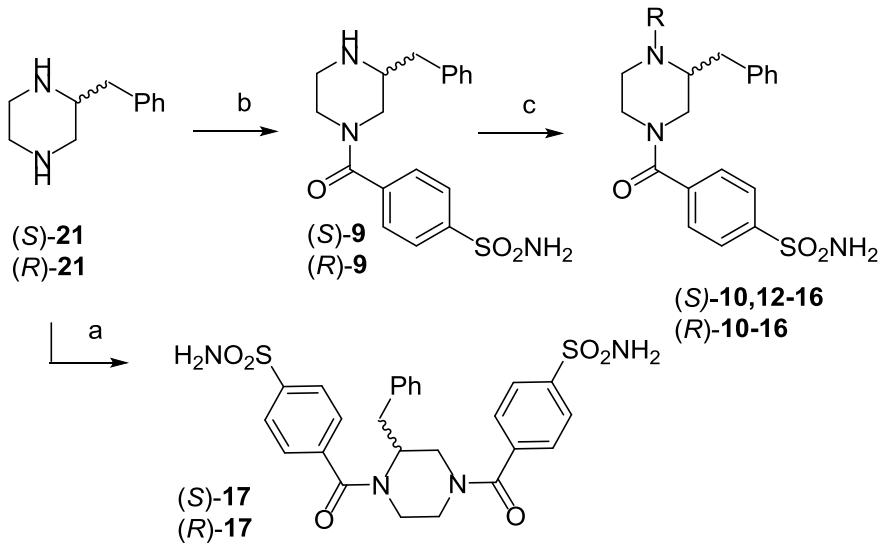

Reagents: (a) 4-Sulfamoylbenzoyl chloride, TEA, acetonitrile; (b) 2,5-dioxopyrrolidin-1-yl 4-sulfamoylbenzoate, CH_3CN; (c) R-Z, base (when necessary), acetonitrile. For the meaning of R-Z and base see Table 3.

Results and discussion

Carbonic Anhydrase Inhibition. The inhibitory activity of the new compounds on hCA isoforms was assessed using a stopped flow CO_2 hydrase assay [25], The ubiquitous cytosolic hCA I and hCA II, the membrane-anchored hCA IV, and the transmembrane, tumor-associated hCA IX were chosen for biological testing. Results are reported in Table 1; the standard sulfonamide inhibitor acetazolamide (AAZ) was used as reference compound.

All the synthesized compounds were able to inhibit the four hCA isoforms, with K_i values ranging from nanomolar to micromolar. The A and B series differ for the position of the ZBG, which in the A series (compounds **1**-**8**) is on the proximal N atom, close to the stereogenic centre, while in the B series (compounds **9**-**16**) is placed on the distal N atom. The position of the ZBG does not clearly influence activity, since compounds belonging to both A and B series are potent

inhibitors. Either alkyl or acyl/sulfonyl groups are well tolerated. These substituents are not essential for activity, at least on hCA I, h-CA II and hCA IV enzymes, since on these isoforms the NH derivatives **2** and **9** display potency in the low nanomolar range. Nevertheless, even if it is difficult to see a clear-cut influence of the characteristics of the N-substituents (alkyl *vs* acyl/sulphonyl, aromatic *vs* aliphatic, or size) on activity, the R^1 and R^2 groups can effectively modulate potency and selectivity, combined with the proper absolute configuration of the piperazine stereogenic centre.

As far as enantioselectivity is concerned, eudismic ratios (ER, defined in Table 1 as the ratio between the K_i of the *S*-enantiomer divided by the K_i of the *R*-one) showed a wide range of values, going from 0.011 [hCA-IX, (*S*)-**1**/(*R*)-**1**] to 146 [hCA-I, (*S*)-**11**/(*R*)-**11**]. Isoforms I and II do not show a clear *S*/*R* preference, thus complicating the interpretation of structure-activity relationships. On the contrary some preference is found on hCA IV and hCA IX for the *R* and *S* absolute configuration, respectively.

By closely looking to the activity of compounds on each isoform, the following structure-activity relationships (SAR) can be inferred. Several compounds are potent inhibitor of hCA I, with K_i values < 10 nM, the most potent ones being (*R*)-**6** (Ki 2.9 nM), (*R*)-**8** (K_i 3.6 nM), and (*R*)-**11** (K_i 3.9 nM). There is not a clear dependence of activity on absolute configuration. High ER values have been found for compounds of both the A and B series, such as **2** (A series, R^2 = H, ER 48), **8** (A series, R^2 = $PhSO_2$, ER 92), **11** (B-series, R^1 = Me, ER 146) and **14** (B-series, R^1 = $PhCH_2CO$, ER 82), the eutomer being the *R*-enantiomer. At variance, for other compounds such as 10 and 17, the eutomer is the *S*-enantiomer. Regarding the bis-sulfonamide **17**, the second SO_2NH_2 group increases activity on the *S*-isomer of compounds **5** and **13** (14 and 5 times, respectively) while it leaves the *R*-one unaffected.

On hCA II the most potent derivative is the bis-sulfonamide (*S*)-**17** (K_i 2 nM), which is 6-times more potent than acetazolamide (K_i 12 nM); several other compounds have K_i values ≤ 10 nM, showing a potency in the same range as the reference compound. Also on this isoform there is not a

clear dependence of activity on absolute configuration. High ER have been found for the N-methyl derivatives of both A and B series, i.e. compounds **3** (A series, ER = 48) and **11** (B series, ER = 61), and for the NH analogue **2** (A series, ER = 33). A second sulfonamide group increases activity on both N-benzoyl analogues (compare **17** with **5** and **13**), the effect being more evident on the S-derivative bearing a distal N-benzoyl group [(S)-**17**, K_i = 2 nM; (S)-**5**, K_i = 61.3].

Apart from compound **5**, for which the ER is lower than 1, on hCA IV all *R*-enantiomers were more active than the *S*-ones. High ER values have been found for the *N*-methyl derivatives **3** and **11** (95 and 86, respectively), for the phenylacetate analogue **14** (B series, ER = 143) and for the methanesulfonyl amide **7** (A series, ER = 36). The most potent compound was the *N*-methyl derivative (*R*)-**11** (B series, K_i 1.7 nM) but almost all *R*-isomers displayed K_i values in the low nM range, showing potency much higher than the reference compound acetazolamide. The *R*-isomers showing lower activity were the benzyl analogue (*R*)-**1** (Ki 66.9 nM) and the benzoyl derivative (*R*)-**5** (Ki 133.4 nM), both belonging to the A series.

Compared to the other isoforms, hCA IX is less sensitive to the activity of the new compounds: only few of them showed potency in the same range as acetazolamide [(*S*)-**1**, K_i = 27.9 nM; (*S*)-**7**: K_i = 31.6 nM; AAZ: K_i = 25 nM], the others being 3-105 times less potent. However, on this isoform all the *S*-enantiomers were equally or more effective inhibitors than the *R*-ones (ER $\leq$ 1), with the exception of the phenylsulfonyl analogue **16** (ER = 4). A high ER value has been found for the *N*-benzyl derivative **1** (A series), for which the *S*-enantiomer was 91 times more potent than the R-one. The methanesulfonyl group was the best substituent in both A and B series [(*S*)-**7** and (*S*) **15**, respectively]. The introduction of a second sulfonamide group on (*R*)-**5** causes a 10-fold reduction of potency, while the effect on (*R*)-**13**, (*S*)-**13** and (*S*)-**5** is marginal.

As far as isoform selectivity is concerned, some compounds showed some selectivity for the hCA-IV; this isoform has been associated to ocular diseases, cancer cell proliferation and other conditions [7, 26, 27]. For instance, on this isoform (*R*)-**10** displays activity 165-, 26- and 182-fold higher than on hCA-I, II and IX, respectively. A similar profile is also shown by (*R*)-**13**, showing a

13-fold selectivity for CA-IV *vs* hCA-I and II, and 414-fold *vs* hCA-IX. Since both hCA-II and IV have been proposed as drug targets for glaucoma, and also hCA-I may have a role in ocular pathologies, compounds (*R*)-**2** and (*R*)-**11** have been selected for in vivo tests, since they are equipotent on I, II and IV isoforms while their activity is > 165 and >335 times lower, respectively, on hCA-IX.

Table 1. Inhibitory activity of the enantiomers of compounds **1-17** on human (h) CA isoforms I, II, IV and IX. The standard sulfonamide inhibitor acetazolamide (AAZ) was used as reference compound.

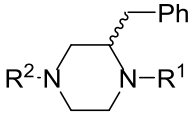

N	**R[1] a)**	**R[2] a)**	**hCA I** K_i (nM)	**ER** b)	**hCA II** K_i (nM)	**ER** b)	**hCA IV** K_i (nM)	**ER** b)	**hCA IX** K_i (nM)	**ER** b)
(S)-**1**	ZBG	**CH_2Ph**	88.9	0.20	46.0	0.26	79.3	1	27.9	0.011
(R)-**1**			455.7		176		66.9		2639.1	
(S)-**2**	ZBG	**H**	421.9	48	264.5	33	75.4	13	93.0	0.06
(R)-**2**			8.7		8.1		5.6		1442	
(S)-**3**	ZBG	**CH_3**	707.0	19	358.6	48	342.5	95	1431.9	1
(R)-**3**			37.7		7.6		3.6		1206.9	
(S)-**4**	ZBG	**CH_3CO**	9.6	0.44	7.7	0.20	6.0	2	170	1
(R)-**4**			21.8		38.9		2.9		197.8	
(S)-**5**	ZBG	**PhCO**	82.8	2	61.3	2	7.8	0.06	227	1
(R)-**5**			44.3		33.4		133.4		205.0	
(S)-**6**	ZBG	**$PhCH_2CO$**	29.5	10	6.8	1	5.4	2	191	1
(R)-**6**			2.9		4.8		2.3		166.1	
(S)-**7**	ZBG	**CH_3SO_2**	186	6	161	21	72.5	36	31.6	0.14
(R)-**7**			29.0		7.5		2.0		232.3	
(S)-**8**	ZBG	**$PhSO_2$**	330.3	92	59.3	8	7.8	2	83.0	0.07
(R)-**8**			3.6		7.6		3.6		1206.9	
(S)-**9**	**H**	ZBG	60.7	1	83.4	5	29.3	6	225.1	0.13
(R)-**9**			49.4		15.4		4.6		1717.9	
(S)-**10**	**CH_2Ph**	ZBG	22.1	0.06	8.3	0.14	73.3	32	249.2	0.59
(R)-**10**			380.2		60.7		2.3		418.5	
(S)-**11**	**CH_3**	ZBG	568.6	146	327.8	61	146	86	1716.3	1
(R)-**11**			3.9		5.4		1.7		1811.1	
(S)-**12**	**CH_3CO**	ZBG	8.8	0.16	7.6	0.24	66.8	20	83.7	0.37
(R)-**12**			55.6		32.0		3.3		227.3	
(S)-**13**	**PhCO**	ZBG	30.7	0.57	15.0	0.29	68.0	17	245	0.15
(R)-**13**			53.9		52.5		4.0		1659.0	
(S)-**14**	**$PhCH_2CO$**	ZBG	542.6	82	92.7	13	371.0	143	177	0.12
(R)-**14**			6.6		7.0		2.6		1520.4	
(S)-**15**	**CH_3SO_2**	ZBG	7.9	0.26	6.0	0.19	79.7	4	74.4	0.41
(R)-**15**			30.6		32.3		19.0		181.1	

(S)-**16**	**$PhSO_2$**	ZBG	245	5	95.1	15	62.2	7	1589.1	4
(R)-**16**			51.6		6.2		8.7		359.6	
(S)-**17**	ZBG	ZBG	6.1	0.11	2.0	0.25	139	27	104	0.04
(R)-**17**			57.2		7.9		5.1		2625.5	
AAZ	-	-	250	-	12	-	74	-	25	-

a) ZBG (Zinc Binding Group): $COC_6H_4SO_2NH_2$; b) ER(eudismic ratio): Ki (S-enantiomer)/Ki (R-enantiomer).

X-ray analysis

To understand the interaction mode of the new derivatives with the enzyme, the X-ray structure of the complex of (*S*)-**17** and (*S*)-**12** bound to hCA I were solved at 1.5 and 1.6 Å resolution, respectively. Compound (*S*)-**17** was selected in order to see which arylsulfonamide group was going to coordinate the Zn ion, and (*S*)-**12**, carrying a small acetyl group, was selected for comparison. Crystal parameters and refinement data are summarized in Table 2. Surprisingly, while the electron density maps unambiguously showed the inhibitor molecules, electron density was almost absent for the second N^4-sulfamoylbenzoyl moiety of (*S*)-**17**, which therefore was not introduced in the model. It should be noted that very few adducts of hCA I with bound inhibitors were reported up until now [28], and this is the reason why we concentrated on this isoform for the compounds reported here.

Both inhibitors place their sulfamoylbenzoyl moiety in a superimposable position and orientation, coordinating the Zn(II) ion by means of the deprotonated sulfonamide moiety (Fig. 1). The sulfonamide nitrogen atoms also make a strong H-bond with the OH of Thr199, while one of the sulfonamide oxygen is engaged in a hydrogen bond with the amide nitrogen of Thr199. These are the usual interactions made by the solfonamide group within the binding site [29], In addition, the benzoyl rings make contacts with His94 and Leu198, and another H-bond is established between the carbonyl oxygen atoms and Asn92.

While the sulfamoylbenzamide moieties of both inhibitors are placed in the same orientation and equivalent position (Fig. 1C), the piperazine rings adopted quite different conformations: a chair for (*S*)-**12** (Fig. 1D), and a twisted boat for (*S*)-**17** (Fig. 1E). These different shapes place the benzyl substituent in a pseudoequatorial arrangement for (*S*)-**17** and in an axial position for (*S*)-**12**. Despite this difference, the benzyl groups are oriented, albeit in slightly different ways, toward the hydrophobic cavity aligned by residues Phe91, Leu131, Ala135, Leu141 and 198, and Pro202 (Fig.

1C). The benzyl moiety of (*S*)-**12**, which is more deeply inserted into the hydrophobic cavity, establishes Van der Waals contacts with Ala135 and Leu131; in addition to these interactions, (*S*)-**17** is able to interact also with Leu141.

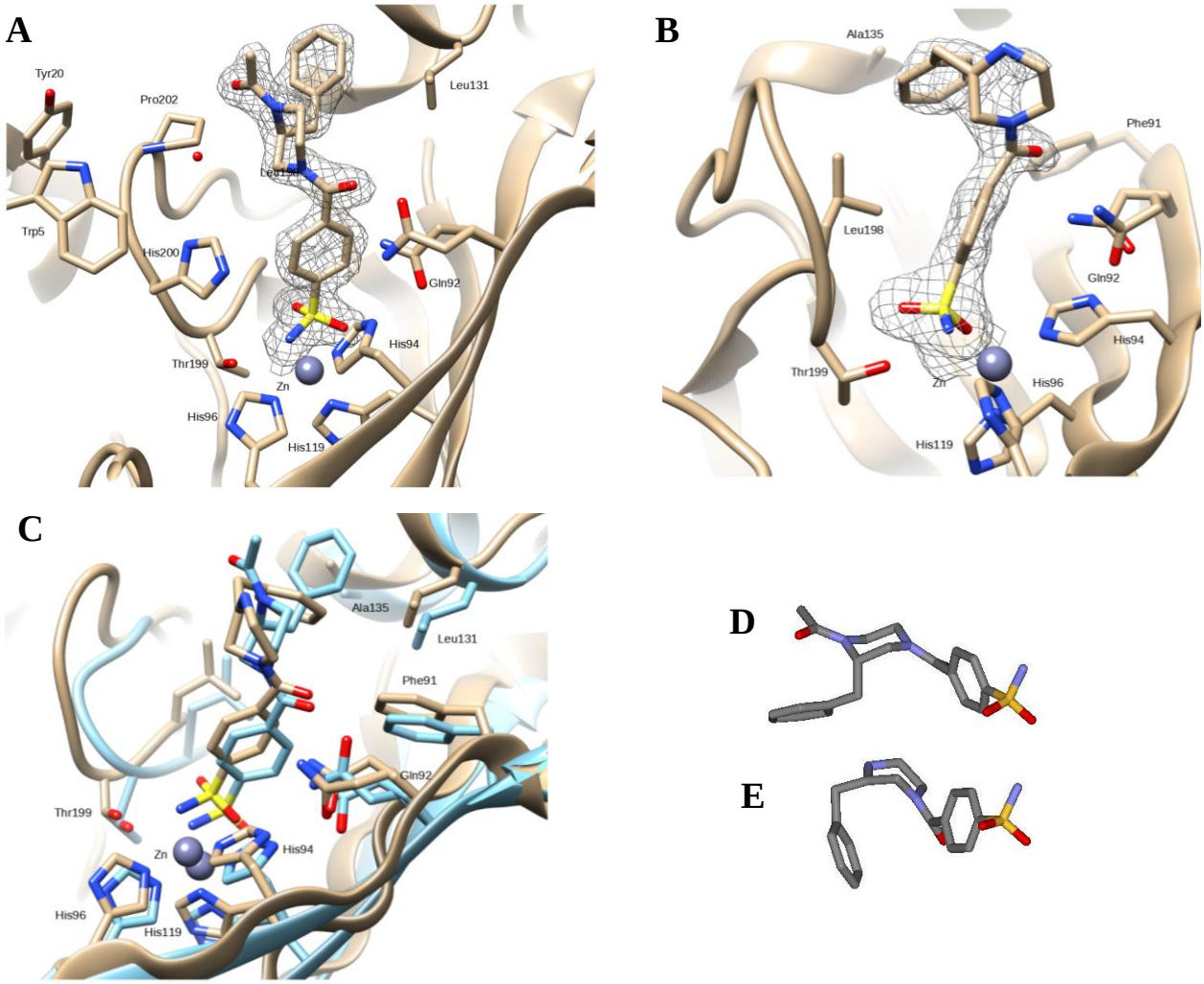

Figure 1. Electronic density for the complex of hCA I with (*S*)-**17** (A) and (*S*)-**12** (B) bound within the active site. The Zn(II) ion (gray sphere), its three histidine ligands (H95, H 97 and H120) as well as amino acid residues involved in the binding of the inhibitor are also evidenced. C) Superimposition of the X-ray structures of hCAI in complex with (*S*)-**17** and (*S*)-**12**. D) Conformation of (*S*)-**12** in the enzyme active site. E) Conformation of (*S*)-**17** in the enzyme active site.

Table 2. Summary of Data Collection and Atomic Model Refinement Statistics.[a]

	HCA-I + (S)-12	**HCA-I + (S)-17**
PDB ID	6EVR	6EX1
Wavelength (Å)	0.966	0.966
Space Group	P212121	P212121

Unit cell (a,b,c) (Å)	62.12, 71.06, 122.12	62.98, 71.47, 120.94
Limiting resolution (Å)	28.5 - 1.5	1.6
Unique reflections	87056 (13980)	72418 (11109)
Rsym (%)	4.9 (65.4)	7.2 (140.5)
R**meas** (%)	5.5 (74.6)	8.6 (169.8)
Redundancy	4.41 (4.42)	3.16 (3.06)
Completeness overall (%)	99.4 (98.0)	98.4 (95.0)
<I/(I)>	13.93 (2.04)	7.27(0.69)
CC (1/2)	99.9 (81.3)	99.1 (51.9)
Refinement statistics		
Resolution range (Å)	20.0 – 1.5	20.0-1.6
Unique reflections, working/free	82483/4378	67693/3617
Rfactor (%)	18.43	21.39
Rfree(%)	22.27	24.64
No. of protein atoms	4043	4038
No. of water molecules	453	320
No. of heterogen atoms	72	64
r.m.s.d. bonds(Å)	0.023	0.006
r.m.s.d. angles (°)	2.151	1.156
Ramachandran statistics (%)		
Most favored	97.3	97.3
additionally allowed	2.7	2.7
outlier regions	0	0
Average B factor (Å^2)		
All atoms	27.31	36.69
inhibitors	25.37	45.52
solvent	38.66	44.34

[a]Values in parentheses are for the highest resolution shell.

Computational studies

The binding mode of the new compounds on hCA II and IV, the isoforms mainly involved in the pathogenesis of glaucoma, was predicted by docking simulations. A small array of regio- and stereo-isomers, namely the N-benzyl derivatives (*S*)-**1**, (*R*)-**1**, (*S*)-**10** and (*R*)-**10**, and *N*-benzoyl amide-bearing (*S*)-**5**, (*R*)-**5**, (*S*)-**13** and (*R*)-**13**, were chosen as representative to evaluate the

influence on the key interactions taking place within hCA II and hCA IV binding pockets. Despite the similar overall fold of CA II and CA IV, some unique structural features mark the differences between the two isozymes which, however, do not involve the catalytic Zn ion region. The polypeptide segment Val131-Asp136 in CA IV arranges in an extended loop conformation rich of charged residues extending to the outside. The corresponding amino acids in CA II, comprising Phe131, are folded as a short α-helix and constitutes part of the well-known lipophilic region of hCA-II binding cavity [30], These marked differences did not prevent the benzenesulfonamide moieties of the selected ligands to orient deeply within the active site region of both the isozymes, where the negatively charged nitrogen atom replaced the zinc-bound nucleophile, the NH is at H-bond distance with T199 OG1 and one oxygen atom of the ZBG accepts a hydrogen bond by the backbone NH of the same residue. Additionally, the aromatic ring showed π-alkyl interactions with Val121, Val135, His94 and Leu198. This wide set of interactions is consistent with the biological results, being all the screened derivatives strong inhibitors of both hCA II and IV with K_i values spanning in the low-medium nanomolar range, and confirms the pattern of interactions found in the crystal structures of (*S*)-**17** and (*S*)-**12** with hCA I.

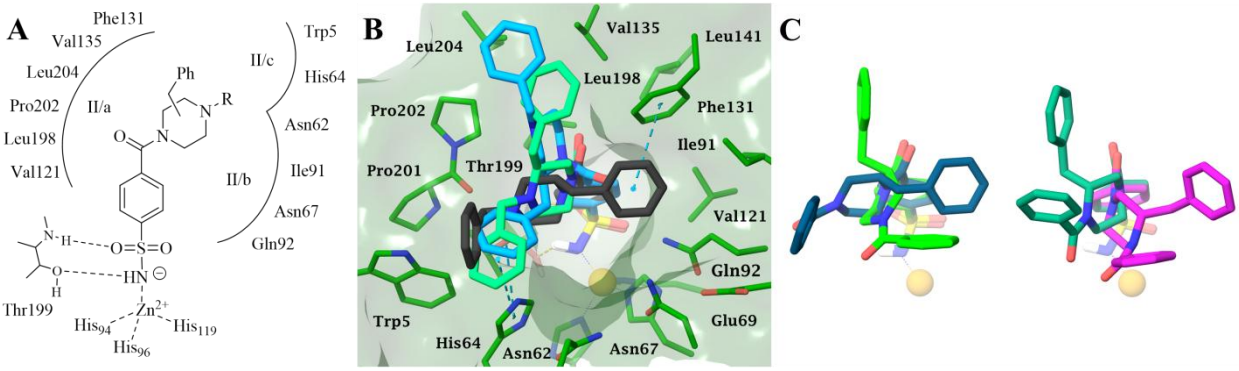

Figure 2. Binding modes of the studied derivatives in the hCA II active site. A) Schematic representation of the sulfonamide zinc binders within hCA II active site. B) Docking poses of compounds (*S*)-**1** (cyan), (*R*)-**1** (black), (*S*)-**10**; C) superposed docked orientations of (*S*)-**5** (green), (*R*)-**5** (blue-green), (*S*)-**13** (magenta), (*R*)-**13** (sea-green).

The arrangement of the benzylpiperazinyl tails within the binding clefts remarks the distinct nature of the residues at the outer rim of hCA II and IV enzymatic cavities. As a result, the two benzylic moieties of derivatives (*S*)-**1**, (*R*)-**1**, (*S*)-**10** and (*R*)-**10** as well as the benzylic and *N*-benzoylic portions of (*S*)-**5**, (*R*)-**5**, (*S*)-**13** and (*R*)-**13** were found to lie within three possible area of hCA-II active site, defined by Phe131, Val135, Leu204, Pro202 (region II/a), Ile91, Gln92, Asn67, Asn62 (region II/b) and Asn62, His64, Trp5 (region II/c), with which form lipophilic and dipole-dipole interactions (Figure 2).

In the hCA IV binding site, the lipophilic portions of most compounds seek to deviate from the charged residues loop, preferentially pointing towards regions formed by residues Gln92, Met67, Gln60, Asn62, His64 (Figure 3), with the *N*-benzoyl and/or benzyl groups of (*S*)-**13,** (*S*)-**5**, (*R*)-**1**, (*R*)-**5**, and (*R*)-**13**, (*R*)-**10** forming wide sets of hydrophobic and/or dipole-dipole interactions. Moreover, the CO of the benzoyl groups acted as acceptor in the H-bond contact with His64 (Figure 3). Conversely, the analysis of poses for compounds (*S*)-**1** and (*S*)-**10** showed that the N-benzyl piperazine moieties oriented towards residues Glu123 and Lys206 forming a charged H-bond involving the protonated piperazine nitrogen and the negatively charged carboxy group of Glu123. In addition, a π-cation interaction with NZ atom of Lys206 stabilized the pose.

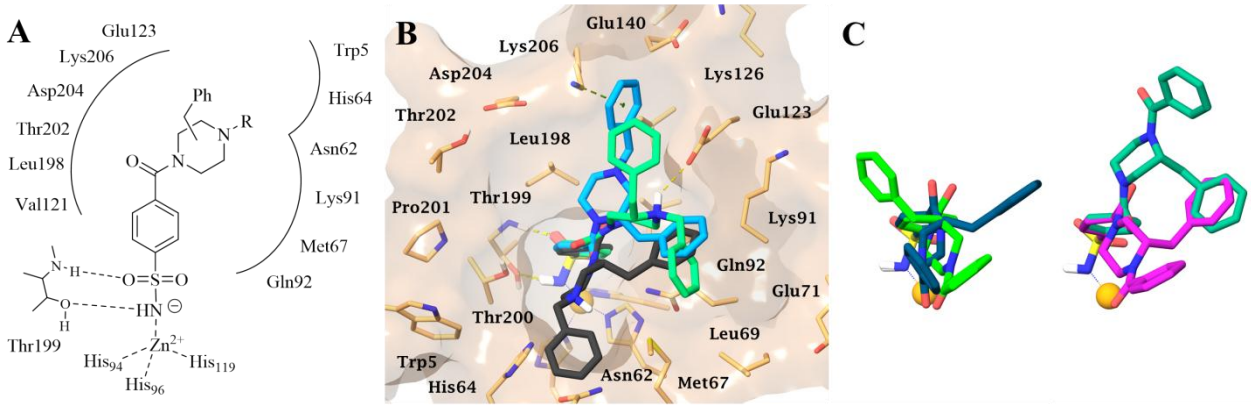

Figure 3. Binding modes of the studied derivatives in the hCA IV active site. A) Schematic representation of the sulfonamide zinc binders within hCA IV active site. B) Docking poses of compounds (*S*)-**1** (cyan), (*R*)-**1** (black), (*S*)-**10** (aquamarine) within hCA II active site; C) superposed docked orientations of (*S*)-**5** (green), (*R*)-**5** (blue-green), (*S*)-**13** (magenta), (*R*)-**13** (sea-green).

It is interesting to note how the stereocenters configuration as well as the positioning of the benzyl moieties on the C2/C3 piperazine carbon atoms differently influenced the orientation of the tails within both binding sites, eliciting varied sets of contacts with the cleft residues, which were comparable as the scoring function values are concerned. At a greater extent, the influence of the stereocenter configuration is evident in case of hCA IV, within whose binding site the orientations of couples of enantiomers, i.e. (*S*)/(R)-**1**, (*S*)/(R)-**10**, (*S*)/(R)-**5** and (*S*)/(R)-**13** almost crossed each other leading to variable trends of non-bonded interactions.

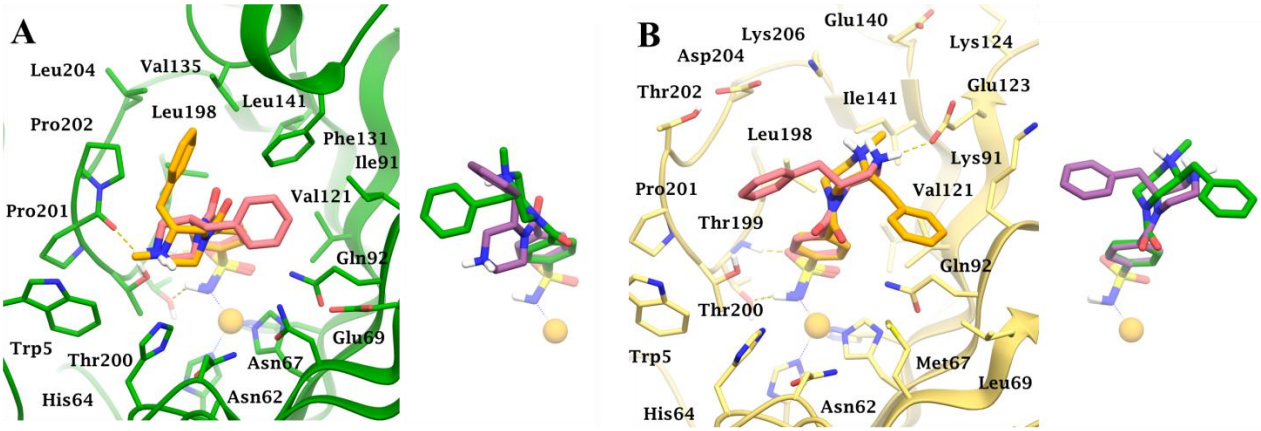

Figure 4. Binding modes of compounds (*R*)-**2** (pink), (*R*)-**11** (orange) (*S*)-**11** (dark green), (*S*)-**2** (violet) within hCA II (A) and hCA IV (B) active site.

The inspection of the docking results of both (*R*)-**2** and (*R*)-**11**, evaluated as anti-glaucoma agents, and their enantiomers (S)-**2** and (S)-**11** suggested a key role played by Glu123 in defining the orientations of the benzyl piperazine within hCA IV binding cavity (Figure 3B). Indeed, the absence of a second bulky substituent at the piperazine *N*-atom allowed the charge mediated interaction between NH_2^+/$NH(CH_3)^+$ group of the heterocycle, regardless the configuration or position of the benzyl moieties (regio-isomers). In hCA II, due to the presence of a lipophilic region in place of the hCA IV charged residues, a wide set of hydrophobic ligand/target contacts are present (Figure 4A) and H-bonds are established between Pro201 backbone CO and the positively charged NH group of piperazine.

Docking scores were not predictive of the activity trends for the computationally investigated derivatives which all exhibit identical coordination geometry of the sulfonamide group to the Zn ion as well as an extended and equipotent sets of interactions within the binding cavities. The accuracy of the used docking protocol was assessed evaluating the ability of the docking in reproducing the geometry of the cocrystallized ligand (S)-**12** within hCA I. The superposed structures (Figure S1, Supporting Information) showed a very good agreement (RMSD value: 0.4608 Å).

***In vivo* IOP testing.**

The intraocular pressure (IOP) lowering properties of the new derivatives (*R*)-**2** and (*R*)-**11** were investigated in a transient animal model of glaucoma. The compounds, used as hydrochloride salts, were formulated as 1% eye drops. High IOP was induced to rabbits by injection of 0.1 mL of hypertonic saline solution (5% in pyrogen free sterile 0.9% NaCl solution) into the vitreous of both eyes. Results, reported in Fig 5A, were compared to dorzolamide hydrochloride (1% solution). The two compounds were able to reduce IOP after 60 min from administration, reaching the maximum activity at 120 min, lowering the pressure of about 10 mmHg. Potency and efficacy were similar to the reference drug dorzolamide.

Compound (*R*)-**2** was tested also in a stable model of glaucoma, obtained through the injection of 0.1 mL of 0.25% carbomer, which induced a sustained ocular hypertension in all tested eyes. Dorzolamide was again used as reference drug. The administration of compound (*R*)-**2** significantly reduced the IOP ($p<0.001$) at 24, 48, 72 and 96 hours in comparison to vehicle (Figure 5B). The effect of both dorzolamide and (*R*)-**2** slightly increased from the first to the fourth day of observation, (*R*)-**2** being significantly more potent than the reference compound Dorzolamide. As a matter of fact, the ΔIOP value produced by (*R*)-**2** was roughly two-fold higher than that produced by the same dose of DRZ.

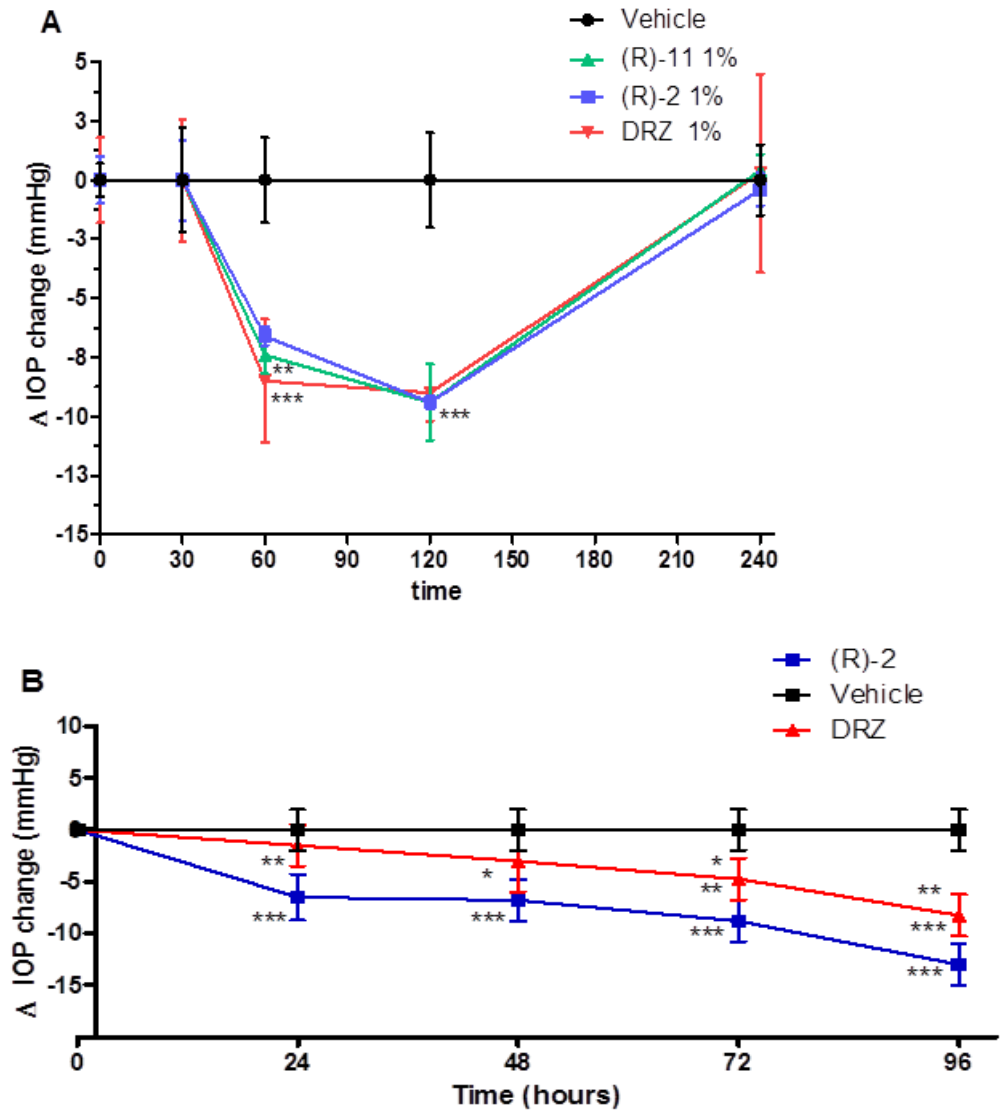

Figure 5. A) Reduction of intra-ocular pressure (IOP, mmHg) versus time (min) in hypertonic saline-induced ocular hypertension in rabbits, after treatment with 0.05 mL of 1% solution of compounds (*R*)-**2** and (*R*)-**11**; dorzolamide (DRZ) was used as reference. Data are analyzed with 2way Anova followed by Bonferroni multiple comparison test. ** p<0.01 (*R*)-**2** and (*R*)-**11** *vs* vehicle at 60'; *** p< 0.001 DRZ *vs* vehicle at 60' at 120'; *** (*R*)-**2** and (*R*)-**11** vs vehicle at 120'.
B) Reduction of intra-ocular pressure (IOP, mmHg) versus time (hours) in stable-induced ocular hypertension in rabbits, 1 hour after instillation of 0.05 mL of 1% solution of compounds (R)-**2**; dorzolamide (DRZ) was used as reference. Data are analyzed with 2way Anova followed by Bonferroni multiple comparison test. *** p<0.001 (*R*)-**2** *vs* vehicle at 24, 48, 72 and 96 hours; ** p< 0.01 DRZ vs vehicle at 72 hours; *** p< 0.001 DRZ vs vehicle at 96 hours; * (*R*)-**2** *vs* DRZ at 48 and 72 hours; ** (*R*)-**2** vs DRZ at 24 and 96 hours.

Conclusions

In this work we reported two new series of enantiopure CA inhibitors, characterized by the presence of a 2- or 3-benzylpiperazine nucleus, carrying on one nitrogen atom a 4-

sulfamoylbenzoyl moiety as Zn-binding group and an alkyl/acyl/sulphonyl moiety on the other one. The compounds were screened against four physiologically relevant CA isoforms (I, II, IV and IX). Several compounds showed K_i values in the low nanomolar range against hCA I, II and IV, and in many instances the activity showed enantioselectivity difference. The hCA I and II isoforms did not show a clear *S*/*R* preference, whereas some enhanced efficacy was found on hCA IV for the *R* enantiomers. The hCA IX isoform was not very sensitive to the new compounds, although some of them show inhibition constants in the same range as acetazolamide, a clinically used drug.

There is not a clear-cut influence of the position of the ZBG and of the characteristics of the N-substituents on activity, which makes difficult to derive SAR for this set of molecules. Nevertheless, the R^1 and R^2 groups effectively modulated potency and selectivity, combined with the proper absolute configuration of the piperazine stereogenic centre. A possible explanation of this come from the study of the binding mode of the new compounds, performed by means of X-ray crystallography on hCA I and molecular modelling on hCA II and IV. While the benzenesulfonamide group is locked in the usual Zn-coordinating position, the rest of the molecule did not bind in a unique way: stereochemistry and flexibility of the piperazine ring allowed different orientations possible, with the tail establishing polar and/or hydrophobic contacts within the binding site, thus strongly stabilizing the enzyme-inhibitor adduct. Two compounds, (*R*)-**2** and (*R*)-**11**, showing high potency on both hCA-II and IV, were tested in an animal model of transient glaucoma, and were found able to lower intraocular pressure, with potency comparable to dorzolamide. In addition, (*R*)-**2** was found more potent than dorzolamide in a stable model of glaucoma. In conclusion, we have found a new series of potent CA inhibitors, displaying some preference for CA II and IV toward IX. These molecules represent a new promising class of antiglaucoma agents. Work is underway to improve potency and selectivity, and to expand structure-activity relationships of this class of compounds.

Experimental section

Chemistry. All melting points were taken on a Büchi apparatus and are uncorrected. NMR spectra were recorded on a Brucker Avance 400 spectrometer (400 MHz for ^{1}H NMR, 100 MHz for ^{13}C). Chromatographic separations were performed on a silica gel column by gravity chromatography (Kieselgel 40, 0.063- 0.200 mm; Merck) or flash chromatography (Kieselgel 40, 0.040-0.063 mm; Merck). Yields are given after purification, unless differently stated. When reactions were performed under anhydrous conditions, the mixtures were maintained under nitrogen. The LC-DAD analyses were carried out on a Agilent 1200 system (Agilent, Palo Alto CA, USA) composed by autosampler, binary pump module, column oven and diode array detector (DAD). The column used was a Luna PFP(2) 50 mm length, 2 mm internal diameter and 3 μm particle size (Phenomenex, Bologna, Italy), at constant flow of 0.25 mL min^{-1}, employing a binary mobile phases elution gradient. The solvents used were 5 mM formic acid in milliQwater solution (solvent A) and methanol (solvent B) according to the elution gradient as follows: initial at 90 % solvent A, which was then decreased to 10 % in 8.0 min, kept for 5.0 min, returned to initial conditions in 0.1 min and maintained for 5.0 min for reconditioning, to a total run time of 18.0 min. The column temperature was maintained at 30 °C and the injection volume was 5 μL. The DAD detector acquired the UV absorption between 210-400 nm. The chromatographic profiles of each analyte (reported in the Supporting Informations) were monitored at 230 nm, that represents the maximum UV absorption for these compounds.

High resolution mass spectrometry (HR-MS) analysis were performed with a Thermo Finnigan LTQ Orbitrap mass spectrometer equipped with an electrospray ionization source (ESI). Analysis were carried out in positive ion mode monitoring protonated molecules, $[M+H]^{+}$ species, and it was used a proper dwell time acquisition to achieve 60,000 units of resolution at Full Width at Half Maximum (FWHM). Elemental composition of compounds were calculated on the basis of their measured accurate masses, accepting only results with an attribution error less than 5 ppm and a not integer RDB (double bond/ring equivalents) value, in order to consider only the protonated species [31]. Compounds were named following IUPAC rules by means of MarvinSketch 18.1.

General procedure for the synthesis of alkyl, acyl or solfonyl derivatives

To a solution of the suitable starting material in 5-20 mL of anhydrous acetonitrile, the suitable reactant was added with a base, when needed. The mixture was kept under stirring for 2 hours, then the solvent was removed under vacuum and the residue was purified with flash chromatography to give the corresponding compound. All the compounds were obtained with a >95% purity (LC), spectroscopic characterization was made by means of ^{1}H-NMR, ^{13}CNMR and MS. Synthetic details are reported in Table 2. By means of this procedure, the compounds below have been prepared.

(*S*) and (*R*)-**4-(2,4-dibenzylpiperazine-1-carbonyl)benzenesulfonamide** (*S*)-**1** and (*R*)-**1**. **[^{1}H]-NMR** (DMSO, mixture of conformers**)** δ: 1.91-2.20 (m, 2H); 2.57-2.74 (dd, 1H, J= 13.2, 10.2 Hz); 2.76-2.92 (m, 1H); 2.94-3.14 (m, 2H); 3.19-3.37 (m, 2H); 3.38-3.49 (m, 0.5H); 3.51-3.63 (m, 1.5H); 4.27-4.35 (m, 0.5H); 4.65-4.74 (bs, 0.5H, CH); 6.67-6.76 (bs, 1H, Ar); 6.94-7.04 (bs, 1H, Ar); 7.05-7.20 (m, 4H, Ar); 7.20-7.43 (m, 6H, Ar), 7.66-7.75 (m, 1H, Ar); 7.76-7.85 (m, 1H, Ar) ppm. **[^{13}C]-NMR** (DMSO, mixture of conformers**)** δ: 35.9 (CH_2Ph); 36.4 (CH_2Ph); 37.9 (C_6); 44.0 (C_6); 50.9 (C_2); 53.4 (C_5); 53.7 (C_5 + C_3); 55.3 (C_3); 57.4 (C_2); 62.3 (NCH_2Ph); 126.0 (CH_{Ar}); 126.3 (CH_{Ar}); 126.6 (CH_{Ar}); 126.8 (CH_{Ar}); 127.2 (CH_{Ar}); 127.6 (CH_{Ar}); 127.7 (CH_{Ar}); 128.7 (CH_{Ar}); 129.4 (CH_{Ar}); 129.7 (CH_{Ar}); 138.4 (C_{Ar}); 138.8 (C_{Ar}); 139.1 (C_{Ar}); 139.8 (C_{Ar}); 144.9 (C_{Ar}); 145.1 (C_{Ar}); 168.2 (CO); 168.9 (CO) ppm. ESI-MS (*m/z)*: 450.2 (M+1) ESI-HRMS (*m/z*) $[M+H]^+$: calculated for $C_{25}H_{28}N_3O_3S$ 450.1846; found 450.1848 for (*S*)-**1** and 450.1843 for (*R*)-**1**.

(*S*) and (*R*)- **4-(2-benzyl-4-methylpiperazine-1-carbonyl)benzene-1-sulfonamide** (*S*)-**3**, (*R*)-**3** **[^{1}H]-NMR** (DMSO, mixture of conformers) δ: 1.78-2.12 (m, 2H); 2.20 (s, 3H, CH_3); 2.61-2.97 (m, 3H); 3.05-3.24 (m, 2H); 3.35-3.48 (m, 0.5H); 3.57-3.68 (m, 0.5H); 4.27-4.38 (m, 0.5H); 4.78-4.89 (m, 0.5H); 6.83-7.02 (m, 2H, Ar); 7.18-7.38 (m, 5H, Ar); 7.43 (s, 2H, SO_2NH_2); 7.64-7.87 (m, 2H, Ar) ppm. ESI-HRMS (*m/z*) $[M+H]^+$: calculated for $C_{19}H_{24}N_3O_3S$ 374.1533; found 374.1529 for (*S*)-**3** and 374.1526 for (*R*)-**3**.

(*S*) and (*R*)-**1-[4-(benzenesulfonyl)-2-benzylpiperazin-1-yl]ethan-1-one** (*S*)-**4**, (*R*)-**4**. **[^{1}H]-NMR** ($CDCl_3$, mixture of conformers) δ: 1.56 (s, 1.5H, CH_3); 2.08 (s, 1.5H, CH_3); 2.13-29 (m, 1H); 2.55-3.18 (m, 3H); 3.20-3.42 (m, 2H); 3.63-4.03 (m, 1H); 4.46-4.72 (m, 1H); 4.73-5.01 (m, 2.5H, SO_2NH_2 + 0.5H); 5.12-5.27 (m, 0.5H); 6.78-6.95 (m, 2H, Ar); 7.07-7.39 (m, 5H); 7.72-7.93 (m, 2H, Ar) ppm. ESI-HRMS (*m/z*) $[M+H]^+$: calculated for $C_{20}H_{24}N_3O_4S$ 402.1482; found 402.1478 for (*S*)-**4** and 402.1483 for (*R*)-**4**.

(*S*) and (*R*)- **4-(4-benzoyl-2-benzylpiperazine-1-carbonyl)benzene-1-sulfonamide** (*S*)-**5**, (*R*)-**5**. **[^{1}H]-NMR** (DMSO, mixture of conformers) δ: 2.62-2.85 (m, 0.5H); 2.86-3.15 (m, 3.5H); 3.35-3.63 (m, 2H); 3.64-3.83 (m, 1H); 4.25-4.55 (m, 1.5H); 4.60-5.03 (m, 0.5H); 6.68-7.04 (m, 2H, Ar); 7.05-7.59 (m, 12H, SO_2NH_2 + Ar); 7.60-7.87 (m, 2H, Ar) ppm. ESI-HRMS (*m/z*) $[M+H]^+$: calculated $C_{25}H_{26}N_3O_4S$ 464.1639; found 464.1632 for (*S*)-**5** and 464.1639 for (*R*)-**5**.

(*S*) and (*R*)-**4-[2-benzyl-4-(2-phenylacetyl)piperazine-1-carbonyl]benzene-1-sulfonamide** (*S*)-**6**, (*R*)-**6**. **[^{1}H]-NMR** (DMSO, mixture of conformers) δ: 2.53-2.64 (m, 1H); 2.65-2.97 (m, 3H); 2.98-3.31 (m, 1.5H); 3.61-3.96 (m, 3H); 4.08-4.43 (m, 2H); 4.48-4.54 (m, 0.2H); 4.73-4.94 (m, 0.3H); 6.68-6.88 (m, 1.5H, Ar); 6.89-7.00 (m, 0.5H, Ar); 7.11-7.33 (m, 10H, Ar); 7.38 (s, 2H, SO_2NH_2); 7.55-7.84 (m, 2H, Ar) ppm. ESI-HRMS (*m/z*) $[M+H]^+$: calculated for $C_{26}H_{28}N_3O_4S$ 478.1795; found 478.1789 for (*S*)-**6** and 478.1800 for (*R*)-**6**.

(*S*) and (*R*)-**4-(2-benzyl-4-methanesulfonylpiperazine-1-carbonyl)benzene-1-sulfonamide** (*S*)-**7**, (*R*)-**7**.**[^{1}H]-NMR** (DMSO, mixture of conformers) δ: 2.62-3.15 (m, 8H); 3.35-3.78 (m, 3.5H); 4.37-4.48 (m, 0.25H); 4.87-4.98 (m, 0.25H); 6.83-7.02 (m, 2H, Ar); 7.05-7.58 (m, 7H, Ar + SO_2NH_2); 7.60-7.88 (m, 2H, Ar) ppm. **[^{13}C]-NMR** (DMSO, mixture of conformers) δ: 34.5 (SO_2CH_3); 35.2 (CH_2); 36.9 (CH_2); 43.1 (CH_2); 45.9 (CH_2); 47.4 (CH_2); 48.6 (CH_2); 49.8 (CH); 56.5 (CH); 126.0 (CH_{Ar}); 126.3 (CH_{Ar}); 127.0 (CH_{Ar}); 127.3 (CH_{Ar}); 127.7 (CH_{Ar}); 128.9 (CH_{Ar}); 130.0 (CH_{Ar}); 138.3 (C_{Ar}); 139.3 (C_{Ar}); 145.1 (C_{Ar}); 168.5 (CO); 169.1 (CO) ppm. ESI-HRMS (*m/z*) $[M+H]^+$: calculated for $C_{19}H_{24}N_3O_5S_2$ 438.1152; found 438.1153 for (*S*)-**7** and 438.1150 for (*R*)-**7**.

(*S*) and (*R*)-**4-[4-(benzenesulfonyl)-2-benzylpiperazine-1-carbonyl]benzene-1-sulfonamide** (*S*)-**8**, (*R*)-**8**. **[^{1}H]-NMR** (DMSO, mixture of conformers) δ: 2.23-2.62 (m, 2H); 2.78-2.93 (m,0.5 H); 2.94-3.14 (m, 1.5H); 3.31-3.43 (m, 1H); 3.43-3.67 (m, 2H); 3.68-3.88 (m, 1H); 4.35-4.48 (m, 0.5H); 4.86-4.93 (m, 0.5H); 6.85-7.04 (m, 2H, Ar); 7.17-7.37 (m, 5H, Ar); 7.41 (s, 2H, SO_2NH_2); 7.58-7.87 (m, 7H, Ar) ppm. **[^{13}C]-NMR** (DMSO, mixture of conformers) δ: 35.1 ($PhCH_2$); 35.4 ($PhCH_2$); 36.9 (CH_2); 42.9 (CH_2); 46.1 (CH_2); 47.8 (CH_2); 48.9 (CH_2); 49.7 (CH); 56.4 (CH); 125.8 (CH_{Ar}); 126.2 (CH_{Ar}); 127.0 (CH_{Ar}); 127.4 (CH_{Ar}); 127.8 (CH_{Ar}); 128.0 (CH_{Ar}); 128.9 (CH_{Ar}); 133.9 (CH_{Ar}); 135.4 (C_{Ar}); 135.7 (C_{Ar}); 138.2 (C_{Ar}); 139.2 (C_{Ar}); 145.0 (C_{Ar} 145.2 (C_{Ar}); 168.5 (CO); 169.1 (CO) ppm. ESI-HRMS (*m/z*) $[M+H]^+$: calculated for $C_{24}H_{26}N_3O_5S_2$ 500.1308; found 500.1312 for (*S*)-**8** and 500.1304 for (*R*)-**8**.

(*S*) and (*R*)-**4-(3-benzylpiperazine-1-carbonyl)benzene-1-sulfonamide** (*S*)-**9**, (*R*)-**9**. **[^{1}H]-NMR** (DMSO, mixture of conformers) δ: 2.52-2.83 (m, 6H); 2.90-3.05 (m, 1H); 3.22-3.30 (m, 1H); 4.17-4.29 (m, 1H); 7.03-7.36 (m, 5H, Ar); 7.44 (s, 2H, Ar); 7.47-7.53 (d, J = 7.2 Hz, 1H, Ar); 7.71-7.77 (m, 0.5H, Ar); 7.78-7.85 (d, J = 6.4 Hz, 0.5 H, Ar) ppm. ESI-HRMS (*m/z*) $[M+H]^+$: calculated for $C_{18}H_{22}N_3O_3S$ 360.1376; found 360.1379 for (*S*)-**9** and 360.1373 for (*R*)-**9**.

(*S*) and (*R*)-**4-(3,4-dibenzylpiperazine-1-carbonyl)benzene-1-sulfonamide** (*S*)-**10**, (*R*)-**10**. **[^{1}H]-NMR** ($CDCl_3$, mixture of conformers) δ: 2.27-2.46 (m, 1H); 2.59-2.64 (m, 2H); 2.83-2.96 (m, 1H); 2.97-3.18 (m, 1.5H); 3.22-3.39 (m, 1.5H); 3.42-3.63 (m, 2H); 3.72-3.82 (m, 0.5H); 3.85-3.97 (m, 0.5H); 3.98-4.18 (m, 1H); 5.53-5.71 (m, 2H, SO_2NH_2); 6.78-6.88 (m, 1H, Ar); 7.03-7.15 (m, 1H, Ar); 7.16-7.49 (m, 9H, Ar); 7.44-7.58 (m, 1H, Ar); 7.62-7.73 (m, 1H, Ar); 7.83-7.91 (m, 1H, Ar) ppm. **[^{13}C]-NMR** ($CDCl_3$, mixture of conformers) δ: 32.5 (CH_2Ph); 33.9 (CH_2Ph); 42.1 (C_2); 44.9 (C_2); 47.5 (C_6); 48.6 (C_6); 49.3 (C_5); 50.5 (C_5); 58.0 (NCH_2Ph); 58.3 (NCH_2Ph); 60.4 (C_3); 61.8 (C_3); 126.3 (CH_{Ar}); 126.6 (CH_{Ar}); 127.4 (CH_{Ar}); 127.5 (CH_{Ar}); 128.0 (CH_{Ar}); 128.5 (CH_{Ar}); 128.6 (CH_{Ar}); 128.8 (CH_{Ar}); 128.9 (CH_{Ar}); 129.3 (CH_{Ar}); 129.6 (CH_{Ar}); 137.9 (C_{Ar}); 138.2 (C_{Ar}); 138.8 (C_{Ar}); 139.0 (C_{Ar}); 139.6 (C_{Ar}); 143.3 (C_{Ar}); 143.5 (C_{Ar}); 168.7 (CO); 138.9 (CO) ppm. ESI-

HRMS (*m/z*) $[M+H]^+$: calculated for $C_{25}H_{28}N_3O_3S$ 450.1846; found 450.1839 for (*S*)-**10** and 450.1847 for (*R*)-**10**.

(*S*) and (*R*)- **4-(3-benzyl-4-methylpiperazine-1-carbonyl)benzene-1-sulfonamide** (*S*)-**11**, (*R*)-**11**. **[^{1}H]-NMR** (DMSO, mixture of conformers) δ: 2.13-2.41 (m, 5.5H, NCH_3+piperazine protons); 2.63-2.97 (m, 2.5H); 2.98-3.32 (m, 3H); 3.77-3.87 (m, 0.5H); 4.03-4.14 (m, 0.5H); 6.93-7.02 (m, 1H, Ar); 7.04-7.17 (m, 1H, Ar); 7.18-7.39 (m, 4H); 7.44 (s, 2H, SO_2NH_2); 7.47-7.58 (m, 1H, Ar); 7.61-7.73 (m, 1H, Ar); 7.80-7.91 (m, 1H, Ar) ppm. ESI-HRMS (*m/z*) $[M+H]^+$:calculated for $C_{19}H_{24}N_3O_3S$ 374.1533; found 374.1532 for (*S*)-**11** and 374.1531 for (*R*)-**11**.

(*S*) and (*R*)-**4-(4-acetyl-3-benzylpiperazine-1-carbonyl)benzene-1-sulfonamide** (*S*)-**12**, (*R*)-**12**. **[^{1}H]-NMR** ($CDCl_3$, mixture of conformers) δ: 1.43-1.56 (bs, 0.5H, CH_3); 1.57-1.72 (bs, 1H, CH_3); 2.02 (s, 1.5H, CH_3); 2.42-2.63 (m, 0.5H); 2.71-3.18 (m, 3.5H); 3.20-3.73 (m, 2H); 3.81-3.93 (bs, 0.5H); 4.02-4.12 (bs, 0.5H); 4.40-4.97 (m, 2H); 5.88 (bs, 2H, SO_2NH_2); 6.83-6.97 (m, 1H, Ar); 7.00-7.38 (m, 4H, Ar); 7.42-7.57 (m, 2H, Ar); 7.78-7.94 (m, 2H, Ar) ppm. **[^{13}C]-NMR** ($CDCl_3$) δ: 20.8 (CH_3); 21.7 (CH_3); 35.2 (CH_2); 35.9 (CH_2); 36.3 (CH_2); 36.7 (CH_2); 41.4 (CH_2); 42.3 (CH_2); 45.0 (CH_2); 47.3 (CH_2); 50.2 (CH); 56.4 (CH); 126.8 (CH_{Ar}); 127.2 (CH_{Ar}); 127.8 (CH_{Ar}); 128.5 (CH_{Ar}); 128.9 (CH_{Ar}); 129.3 (CH_{Ar}); 136.6 (C_{Ar}); 137.2 (C_{Ar}); 138.9 (C_{Ar}); 144.0 (C_{Ar}); 169.6 (CO); 170.0 (CO) ppm. ESI-HRMS (*m/z*) $[M+H]^+$: calculated for $C_{20}H_{24}N_3O_4S$ 402.1482; found 402.1488 for (*S*)-**12** and 402.1474 for (*R*)-**12**.

(*S*) and (*R*)-**4-(4-benzoyl-3-benzylpiperazine-1-carbonyl)benzene-1-sulfonamide** (*S*)-**13**, (*R*)-**13**. **[^{1}H]-NMR** (DMSO, mixture of conformer) δ: 2.82-3.08 (m, 4H); 3.36-3.62 (m, 1.5H); 3.63-3.93 (m, 1H); 4.15-4.52 (m, 2H); 4.72-5.02 (m, 0.5H); 6.58-6.96 (m, 2H, Ar); 6.97-7.39 (m, 8H, Ar); 7.46 (s, 2H, SO_2NH_2); 7.53-7.77 (m, 2H, Ar); 7.78-7.93 (m, 2H, Ar) ppm. ESI-HRMS (*m/z*) $[M+H]^+$: calculated for $C_{25}H_{26}N_3O_4S$ 464.1639; found 464.1633 for (*S*)-**13** and 464.1642 for (*R*)-**13**.

(*S*) and (*R*)-**4-[3-benzyl-4-(2-phenylacetyl)piperazine-1-carbonyl]benzene-1-sulfonamide** (*S*)-**14**, (*R*)-**14**. **[^{1}H]-NMR** (DMSO, mixture of conformers) δ: 2.51-2.62 (m, 0.5H); 2.65-3.12 (m, 6H);

3.35-3.52 (m, 1H); 3.53-3.67 (m, 1H); 4.05-4.53 (m, 2H); 4.55-4.85 (m, 0.5H); 6.72-6.95 (m, 1H, Ar); 6.96-7.03 (m, 1H, Ar); 7.05-7.33 (m, 8H, Ar); 7.42 (s, 2H, SO_2NH_2); 7.52-7.72 (bs, 2H, Ar); 7.78-7.93 (m, 2H, Ar) ppm. ESI-HRMS (*m/z*) $[M+H]^+$: calculated for $C_{26}H_{28}N_3O_4S$ 478.1795; found 478.1786 for (S)-**14** and 478.1802 for (*R*)-**14**.

(*S*) and (*R*)-**4-(3-benzyl-4-methanesulfonylpiperazine-1-carbonyl)benzene-1-sulfonamide** (*S*)-**15**, (*R*)-**15**. **[^{1}H]-NMR** (CD_3OD, mixture of conformers) δ: 2.37-2.72 (m, 3H); 2.93-3.13 (m, 2H); 3.37-3.73 (m, 5H); 4.12-4.23 (m, 0.5H, CH); 4.25-4.47 (m, 0.5H, CH); 4.51-4.68 (m, 1H); 7.02-7.41 (m, 5H, Ar); 7.54-7.68 (m, 2H, Ar); 7.93-8.08 (m, 2H, Ar) ppm. ESI-HRMS (*m/z*) $[M+H]^+$: calculated for $C_{19}H_{24}N_3O_5S_2$ 438.1152; found 438.1148 for (*S*)-**15** and 438.1160 for (*R*)-**15**.

(*S*) and (*R*)- **4-[4-(benzenesulfonyl)-3-benzylpiperazine-1-carbonyl]benzene-1-sulfonamide** (*S*)-**16**, (*R*)-**16**. **[^{1}H]-NMR** (DMSO, mixture of conformers) δ: 2.53-2.66 (m, 1H); 2.68-2.83 (m, 1.5H); 2.84-2.91 (m, 0.5H), 2.92-3.08 (m, 0.5H); 3.11-3.29 (m, 2H), 3.40-3.53 (m, 0.5H); 3.55-3.74 (m, 1H); 4.09-4.47 (m, 2H); 6.86-7.02 (bs, 0.5H, Ar); 7.05-7.38 (m, 3.5H, Ar); 7.42-7.79 (m, 10H, Ar +SO_2NH_2); 7.80-7.95 (m, 2H, Ar) ppm. ESI-HRMS (*m/z*) $[M+H]^+$: calculated for $C_{24}H_{26}N_3O_5S_2$ 500.1308; found 500.1310 for (*S*)-**16** and 500.1304 for (*R*)-**16**.

(*S*) and (*R*)-**4-[2-benzyl-4-(4-sulfamoylbenzoyl)piperazine-1-carbonyl]benzene-1-sulfonamide** (*S*)-**17**, (*R*)-**17**.**[^{1}H]-NMR** (DMSO, mixture of conformers) δ: 2.57-2.89 (m, 1H); 2.90-3.21 (m, 2.5H); 3.30-3.88 (m, 3.5H); 4.22-4.53 (m, 1.5H); 4.58-5.02 (m, 0.5H); 6.73-7.05 (m, 2H, Ar); 7.08-7.40 (m, 5.5H, Ar); 7.45 (bs, 4H, SO_2NH_2); 7.58-7.98 (m, 5.5H, Ar) ppm. ESI-HRMS (*m/z*) $[M+H]^+$: calculated for $C_{25}H_{27}N_4O_6S_2$ 543.1367; found 543.1360 for (*S*)-**17** and 543.11363 for (*R*)-**17**.

(*S*) and (*R*)-**4-(2-benzylpiperazine-1-carbonyl)benzenesulfonamide (*S*)-2, (*R*)-2**

A solution of acetyl chloride (0.163 mL; 2.28 mmol) in MeOH (10 mL) was added to a suspension of (S)-**1** (514 mg; 1.14 mmol) in MeOH (10 mL). The resulting solution was hydrogenated at 75 psi

over Pd 10%/C (200 mg) for 24 h, then the catalyst was filtered off. Diethyl ether was slowly added to the solution, producing the precipitation of a white solid, which was filtered and treated with a saturated solution of $NaHCO_3$ and extracted three times with ethyl acetate. The organic phase was dried (Na_2SO_4) and the solvent was removed under vacuum to give the title compounds as a white solid. Yield 100%. M.P. 212-216°C. The R-enantiomer (*R*)-**2** was prepared in the same way starting from (*R*)-**1**; chemical and physical characteristics are the same as its enantiomer. **[^{1}H]-NMR** (DMSO, mixture of conformers) δ: 2.57-2.88 (m, 4H); 2.90-3.20 (m, 3.5H); 3.44-3.55 (bs, 0.5H); 4.16-4.27 (m, 0.5H); 4.67-4.74 (bs, 0.5 H); 6.82-6.95 (m, 2H, Ar); 7.14-7.33 (m, 5H, Ar); 7.35-7.44 (s, 2H, SO_2NH_2); 7.63-7.85 (m, 2H, Ar) ppm. **[^{13}C]-NMR** (DMSO, mixture of conformers) δ: 34.7 (CH_2Ph); 35.2 (CH_2Ph); 39.1 (CH_2); 44.1 (CH_2); 45.6 (CH_2); 47.0 (CH_2); 48.3 (CH_2); 49.9 (CH); 57.0 (CH); 125.9 (CH_{Ar}); 126.7 (CH_{Ar}); 127.0 (CH_{Ar}); 127.4 (CH_{Ar}); 128.7 (CH_{Ar}); 129.6 (CH_{Ar}); 129.7 (CH_{Ar}); 138.9 (C_{Ar}); 139.8 (C_{Ar}); 144.7 (C_{Ar}); 168.3 (CO); 169.1 (CO) ppm. ESI-HRMS (*m/z*) $[M+H]^+$: calculated for $C_{18}H_{22}N_3O_3S$ 360.1376; found 360.1374 for (*S*)-**2** and 360.1373 for (*R*)-**2**.

(*S*)-**2,4-dibenzyl-1-methylpiperazine (*S*)-19**

To a stirring solution of (*S*)-**18** (0.115 mg; 0.43 mmol) in absolute EtOH (5 mL), formaldehyde (0.06 mL; 2.2 mmol) and formic acid (0.28 mL; 7.3 mmol) were added. The mixture was then heated at 80°C for 6 hours, then the solvent was removed and the residue was partitioned between DCM and a solution of $NaHCO_3$. Dehydration (Na_2SO_4) and removal of the solvent gave (*S*)-**19** as a yellow oil. Yield 99%. **[^{1}H]-NMR** ($CDCl_3$) δ: 2.0-2.1 (m, 1H); 2.21-2.29 (m, 1H); 2.32-2.41 (m, 1H); 2.43 (s, 3H, NCH_3); 2.44-2.62 (m, 4H); 2.75-2.8 (dt, J= 11.6 Hz, 3.6 Hz, 1H); 3.06-.3.09 (d, J = 11.6 Hz, 1H); 3.24-3.28 (d, J= 13.0 Hz,1H); 3.51-3.55 (d, J= 13.0 Hz, 1H); 7.1-7.33 (m, 10H, Ar) ppm. ESI-MS (*m/z)*: 281.1 $[M+H]^+$.

(*S*)-**2-benzyl-1-methylpiperazine (*S*)-20**

To a solution of (*S*)-**19** (120 mg; 0.43 mmol) in MeOH (10 mL) a solution of acetyl chloride (0.061 ml; 0.86 mmol) in MeOH (10 mL) was added. The resulting mixture was hydrogenated at 75 psi

over Pd 10%/C for 24 hours, then the catalyst was filtered off. The solvent was removed under vacuum and the residue was treated with a saturated solution of $NaHCO_3$ and extracted three times with DCM. The organic phase was dried (Na_2SO_4) and the solvent was removed under vacuum. The residue was purified with flash chromatography (DCM/MeOH/NH_3 90:10:1) to give (*S*)-**20** [21] as a yellow oil. Yield 40%. **[^{1}H]-NMR** ($CDCl_3$) δ: 1.62 (bs, 1H, NH); 2.20-2.29 (m, 2H, H_2 + H_6); 2.37-2.48 (m, 5H, CH_3 + H_3+ C*H*HPh); 2.69-2.75 (dd, J= 12.4, 2.4 Hz; 1H, H_3); 2.78–2.83 (dt, J= 11.6, 2.8 Hz, 1H, H_6); 2.87-2.92 (m, 2H, H_5); 3.13-3.19 (dd, J= 13.2, 4.0 Hz, 1H, CH*H*Ph); 7.12-7.29 (m, 5H, Ar) ppm. **[^{13}C]-NMR** ($CDCl_3$) δ: 36.9 (CH_2Ph); 43.5 (CH_3); 46.1 (C_5); 50.4 (C_3); 56.6 (C_6); 64.9 (C_2); 126.1 ($C_{4'}$); 128.3 ($C_{2'}$ + $C_{6'}$); 19.3 ($C_{3'}$+$C_{5'}$); 139.1 ($C_{1'}$) ppm. ESI-MS (*m/z)*: 191.1 $[M+H]^+$.

Table 3. Details related to the general synthetic procedure.

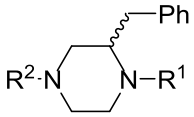

N	R^1	R^2	Reagent (mmol)	R-Z (eq)	Base (eq)	Yield %	Eluent [a]	M.P. (°C)
(*S*)-1	ZBG	CH_2Ph	(*S*)-**18** (1)	ZBG-Cl (1)	TEA (1.2)	79		118-122
(*R*)-1			(*R*)-**18** (1)					120-122
(*S*)-3	ZBG	CH_3	(*S*)-**2** (0.1)	CH_3I (0.5)	-	32	A	> 260
(*R*)-3			(*R*)-**2** (0.1)			41		> 260
(*S*)-4	ZBG	CH_3CO	(*S*)-**2** (0.1)	Ac_2O (5)	-	98	B	202-205
(*R*)-4			(*R*)-**2** (0.1)			99		200-204
(*S*)-5	ZBG	PhCO	(*S*)-**2** (0.1)	PhCOCl (2)	TEA (2)	68	B	> 260
(*R*)-5			(*R*)-**2** (0.1)			92		> 260
(*S*)-6	ZBG	$PhCH_2CO$	(*S*)-**2** (0.1)	$PhCH_2CO$-NHS [b] (3)	-	87	B	180-182
(*R*)-6			(*R*)-**2** (0.1)			68		185-188
(*S*)-7	ZBG	CH_3SO_2	(*S*)-**2** (0.1)	CH_3SO_2Cl (2)	TEA (1.2)	78	C	> 260
(*R*)-7			(*R*)-**2** (0.1)			91		> 260
(*S*)-8	ZBG	$PhSO_2$	(*S*)-**2** (0.1)	$PhSO_2Cl$ (2)	TEA (1.2)	75	B	> 260
(*R*)-8			(*R*)-**2** (0.1)			98		> 260
(*S*)-9	H	ZBG	(*S*)-**21** (0.7)	ZBG-NHS (0.7) [c]	-	70	A	190 (d)
(*R*)-9			(*R*)-**21** (0.8)			74		195 (d)
(*S*)-10	CH_2Ph	ZBG	(*S*)-**9** (0.1)	$PhCH_2Br$ (1.5)	$NaHCO_3$ (10)	69	B	160-162
(*R*)-10			(*R*)-**9** (0.1)			57		156-159
(*S*)-11	CH_3	ZBG	(*S*)-**20** (0.15)	ZBG-Cl (1.5)	TEA (1.2)	35	A	197-199
(*R*)-11			(*R*)-**9** (0.2)	CH_3I (0.5)	-	40		201-203
(*S*)-12	CH_3CO	ZBG	(*S*)-**9** (0.1)	Ac_2O (5)	-	85	B	202-205
(*R*)-12			(*R*)-**9** (0.1)			95		201-204

(*S*)-13	PhCO	ZBG	(*S*)-**9** (0.1)	PhCOCl (2)	TEA (3)	80	B	228-231
(*R*)-13			(*R*)-**9** (0.1)			85		230-232
(*S*)-14	$PhCH_2CO$	ZBG	(*S*)-**9** (0.1)	$PhCH_2CO$-NHS[d] (2)	-	38	C	178-180
(*R*)-14			(*R*)-**9** (0.1)			72		170-173
(*S*)-15	CH_3SO_2	ZBG	(*S*)-**9** (0.1)	CH_3SO_2Cl (1)	TEA (1.2)	82	C	189-192
(*R*)-15			(*R*)-**9** (0.1)			78		195-197
(*S*)-16	$PhSO_2$	ZBG	(*S*)-**9** (0.1)	$PhSO_2Cl$ (2)	TEA (3)	82	B	203-206
(*R*)-16			(*R*)-**9** (0.1)			91		210-212
(*S*)-17	ZBG	ZBG	(*S*)-**21** (0.16)	ZBG-Cl (2)	TEA (3)	99	B	>260
(*R*)-17			(*R*)-**21** (0.16)			99		> 260

[a]**A:** DCM/MeOH/NH_3 95:5:0.5; **B:** DCM/MeOH 95:5; **C:** DCM/MeOH 93:7. [b] Prepared as reported in ref [20] [c] Addition performed at 0°C. [d] Prepared as reported in ref [23]. ZBG: $COC_6H_4SO_2NH_2$; ZBG-NHS: 2,5-dioxopyrrolidin-1-yl 4-sulfamoylbenzoate; $PhCH_2CO$-NHS: 2,5-dioxopyrrolidin-1-yl 2-phenylacetate.

CA inhibition

An Sx.18Mv-R Applied Photophysics (Oxford, UK) stopped-flow instrument has been used to assay the catalytic activity of various CA isozymes for CO_2 hydration reaction [25]. Phenol red (at a concentration of 0.2 mM) was used as indicator, working at the absorbance maximum of 557 nm, with 10 mM Hepes (pH 7.5) as buffer, and 0.1 M Na_2SO_4 (for maintaining constant ionic strength, which is not inhibitory against these isoforms) following the CA-catalyzed CO_2 hydration reaction for a period of 10 s at 25 °C. The CO_2 concentrations ranged from 1.7 to 17 mM for the determination of the kinetic parameters and activation constants. For each inhibitor at least six traces of the initial 5-10% of the reaction have been used for determining the initial rate of the reaction. The uncatalyzed rates were determined in the same manner and subtracted from the total observed rates. Stock solutions of inhibitors (10 mM) were prepared in distilled-deionized water with eventually 3-5 % DMSO, and the dilution up to 0.1 nM were then done using the assay buffer. Inhibitor and enzyme solutions were pre-incubated together for 15 min (standard assay at room temperature) prior to assay, in order to allow for the formation of the enzyme – inhibitor complex. The inhibition constant (K_I), was obtained by considering the classical Michaelis–Menten equation and the Cheng-Prusoff algorithm by using non-linear least squares fitting as reported earlier [32-36]

.

Co-crystallization and X-ray data collection

Crystals of hCA I complexed with compounds (*S*)-**17** and (*S*)-**12** were obtained using the sitting drop vapor diffusion method. 2 µL of 10 mg/ml solution of hCA I in Tris-HCl 20 mM pH 9.0 were mixed with 2 µL of a solution of 28-31% PEG4000, 0.2 M Sodium acetate, 0.1 M Tris pH 8.5-9.0 and were equilibrated against the same solution at 296 K. Crystals of the protein grew in fifteen days. Afterwards hCAI crystals were soaked in 5 mM inhibitor solutions for 3 days.

The crystals were flash-frozen at 100K using a solution obtained by adding 15% (v/v) glycerol to the mother liquor solution as cryoprotectant. Data on crystals of the complexes were collected using synchrotron radiation at the ID30A-1 beamline at ESRF (Grenoble, France) with a wavelength of 0.966 Å and a PILATUS3 2M Dectris CCD detector. Data were integrated and scaled using the program XDS [37]. Data processing statistics are showed in Table 2.

The crystal structure of hCA I (PDB accession code: 1JV0) without solvent molecules and other heteroatoms was used to obtain initial phases of the structures using Refmac5 [38]. 5% of the unique reflections were selected randomly and excluded from the refinement data set for the purpose of Rfree calculations. The initial |Fo - Fc| difference electron density maps unambiguously showed the inhibitor molecules. However electron density was almost absent for the 4-sulfamoylbenzoyl piperazine substituent of the (*S*)-**17** inhibitor which was not introduced in the model.

Atomic models for inhibitors were calculated and energy minimized using the program JLigand 1.0.40 [39]. Refinements proceeded using normal protocols of positional, isotropic atomic displacement parameters alternating with manual building of the models using COOT [40]. Solvent molecules were introduced automatically using the program ARP [41]. The quality of the final models were assessed with COOT and RAMPAGE [42]. Crystal parameters and refinement data are summarized in Table 2. Atomic coordinates were deposited in the Protein Data Bank (PDB accession code: 6EVR and 6EX1). Graphical representations were generated with Chimera [43].

Computational studies

1ZNC chain A was taken and prepared for docking simulations as it was characterized by better crystallographic parameters (i.e. B factors and electronic density maps) than chain B. Thus, 5LJT (hCA II) [44] and 1ZNC-A (hCA IV) [30] crystal structures were prepared according to the Protein Preparation module in Maestro - Schrödinger suite, assigning bond orders, adding hydrogens, deleting water molecules, and optimizing H-bonding networks. Finally, energy minimization with a root mean square deviation (RMSD) value of 0.30 was applied using an Optimized Potentials for Liquid Simulation (OPLS_2005) force field [45].

3D ligand structures were prepared by Maestro [45a], evaluated for their ionization states at pH 7.4 ± 0.5 with Epik [45b]. OPLS-2005 force field in Macromodel [45c] was used for energy minimization for a maximum number of 2500 conjugate gradient iterations and setting a convergence criterion of 0.05 kcal $mol^{-1}Å^{-1}$. Grids for docking were centred in the centroid of the complexed ligand. Flexible docking studies were carried out with the program Glide, using the standard precision (SP) mode, turning on the sampling of ring conformation option and the post-docking minimization [45d]. The best scored docking poses were selected and passed onto Prime for refinement with the VSGB continuum solvent model [45e][46].

IOP experiments

The experimental procedures were carried out in male albino SPF (specific pathogen free) New Zealand rabbits. We followed the Resolution of the Association for Research in Vision and Ophthalmology, the Good Laboratory Practice for the use of animals upon the authorization of Italian regulation on protection of animals (DM 116/1992), in agreement with the European Union Regulations (OJ of ECL 358/1, 12/12/1986). Male albino rabbits (body weight 2-2.5 kg) were kept in individual cages, food and water was provided ad libitum. The animals were maintained on a 12-12h light/dark cycle in a temperature controlled room (22°-23°C).

Animals were identified with a tattoo in the ear, numbered consecutively and examined before the beginning of the study to verify the good general and ophthalmic health condition.

All the compounds were dissolved in pyrogen free sterile 0.9% NaCl solution (i.e. physiologic solution) and 2% DMSO, at 1% concentration. Vehicle was 0.9%NACl+ 2% DMSO. The viability of various compounds was always evaluated after repeated administration using the Draize Eye Test [47].

Topical delivery into the conjunctival cul-de-sac is the most common route of ocular drug delivery. All the compounds were given prior to saline injection for the transient model of glaucoma. The IOP was measured at the very beginning of the experimental session to establish basal IOP. Transient ocular hypertension was induced by the injection of 0.05 mL of sterile hypertonic saline (5%) into the vitreous bilaterally with local anaesthesia provided by one drop of 0.2% oxybuprocaine hydrochloride in each eye one minute before. IOP was measured using a Model 30™ Pneumatonometer (Reichert Inc. Depew, NY) 10 minutes after hypertonic saline injection to verify the rise of IOP into the suitable experimental range (IOP >30 and < 55 mmHg) and after 60, 90, 120, 240 minutes in all groups after drug or vehicle treatment. One drop of 0.2% oxybuprocaine hydrochloride was instilled in each eye immediately before each set of pressure measurements.

Stable ocular hypertension was induced throughout carbomer (Siccafluid, Famila THEA Pharmaceutical, Milan, Italy) injection into the anterior chamber. After the instillation of 0.2% oxybuprocaine hydrochloride (Novesine, Sandoz, Varese, Italy), aqueous humour (about 100 µL) was withdrawn from the anterior chamber of each eye at baseline, before carbomer injection. After that, 0.1 ml of 0.25% carbomer was injected into the anterior chamber by a 25 gauge needle through the corneal limbus [48]. Ocular examination was performed every day. After instillation in each eye of 0.2% oxybuprocaine hydrochloride, IOP was measured before carbomer injection (baseline), two times a day until IOP stabilization, and then, every 24 hours, before and 1 hour after compound

instillation. All IOP measurements were done by two independent investigators using the same pneumatonometer.

Acknowledgment

This work was supported by grants from the University of Florence (Fondo Ricerca Ateneo RICATEN16). The X-ray diffraction experiments were performed on beamline MASSIF-1 at the European Synchrotron Radiation Facility (ESRF), Grenoble, France. We are grateful to Local Contact at the ESRF for providing assistance in using beamline MASSIF-1.

Accession Codes

Coordinates and structure factors for hCA I complexes with (*S*)-**12** and (*S*)-**17** have been deposited in the Protein Data Bank (PDB), accession code: 6EVR and 6EX1). Authors will release the atomic coordinates and experimental data upon article publication.

References

[1] C.T. Supuran, Carbonic anhydrases: novel therapeutic applications for inhibitors and activators, Nature Rev. Drug Discov., 7 (2008) 168-181.

[2] C.T. Supuran, G. De Simone, Carbonic Anhydrases: An Overview, in: G. De Simone, Claudiu T Supuran (Eds.) Carbonic Anhydrases as Biocatalysts - From Theory to Medical and Industrial Applications, Elsevier, Amsterdam, 2015.

[3] C.T. Supuran, Structure-based drug discovery of carbonic anhydrase inhibitors, J. Enzyme Inhib. Med. Chem., 27 (2012) 759-772.

[4] C.T. Supuran, Carbonic anhydrase inhibitors, Bioorg. Med. Chem. Lett., 20 (2010) 3467-3474.

[5] K. Cholkar, H.M. Trinh, D. Pal, A.K. Mitra, Discovery of novel inhibitors for the treatment of glaucoma, Expert Opini. Drug Discov., 10 (2015) 293-313.

[6] A.D. Vadlapudi, A. Patel, K. Cholkar, A.K. Mitra, Recent Patents on Emerging Therapeutics for the Treatment of Glaucoma, Age Related Macular Degeneration and Uveitis, Recent Pat. Biomed. Eng., 5 (2012) 83-101.

[7] A. Waheed, W.S. Sly, Membrane Associated Carbonic Anhydrase IV (CA IV): A Personal and Historical Perspective, in: S.C. Frost, R. McKenna (Eds.) Carbonic Anhydrase: Mechanism, Regulation, Links to Disease, and Industrial Applications, Springer Netherlands, Dordrecht, 2014, pp. 157-179.

[8] S. Strong, G. Liew, M. Michaelides, Retinitis pigmentosa-associated cystoid macular oedema: pathogenesis and avenues of intervention, Br. J. Ophthalmol., 101 (2017) 31-37.

[9] E. Ruusuvuori, K. Kaila, Carbonic Anhydrases and Brain pH in the Control of Neuronal Excitability, in: S.C. Frost, R. McKenna (Eds.) Carbonic Anhydrase: Mechanism, Regulation, Links to Disease, and Industrial Applications, Springer Netherlands, Dordrecht, 2014, pp. 271-290.

[10] Supuran, C. T. Carbonic anhydrase and metabolism, Metabolites, 8 (2018) E25.

[11] C.T. Supuran, Carbonic Anhydrase Inhibition and the Management of Hypoxic Tumors, Metabolites, 7 (2017) 48.

[12] C.T. Supuran, Carbonic anhydrase inhibition and the management of neuropathic pain, Expert Rev. Neurother., 16 (2016) 961-968.

[13] O. Ozensoy Guler, C. Capasso, C.T. Supuran, A magnificent enzyme superfamily: carbonic anhydrases, their purification and characterization, J. Enzyme Inhib. Med. Chem., 31 (2016) 689-694.

[14] M. Shaquiquzzaman, G. Verma, A. Marella, M. Akhter, W. Akhtar, M.F. Khan, S. Tasneem, M.M. Alam, Piperazine scaffold: A remarkable tool in generation of diverse pharmacological agents, Eur. J. Med. Chem., 102 (2015) 487-529.

[15] C. Congiu, V. Onnis, A. Deplano, G. Balboni, N. Dedeoglu, C.T. Supuran, Synthesis of sulfonamides incorporating piperazinyl-ureido moieties and their carbonic anhydrase I, II, IX and XII inhibitory activity, Bioorg. Med. Chem. Lett., 25 (2015) 3850-3853.

[16] J. Sławiński, K. Szafrański, D. Vullo, C.T. Supuran, Carbonic anhydrase inhibitors. Synthesis of heterocyclic 4-substituted pyridine-3-sulfonamide derivatives and their inhibition of the human cytosolic isozymes I and II and transmembrane tumor-associated isozymes IX and XII, Eur. J. Med. Chem., 69 (2013) 701-710.

[17] C. Congiu, V. Onnis, A. Deplano, G. Balboni, M. Ceruso, C.T. Supuran, Synthesis and carbonic anhydrase I, II, IX and XII inhibitory activity of sulfamates incorporating piperazinyl-ureido moieties, Bioorg. Med. Chem., 23 (2015) 5619-5625.

[18] E. Havránková, J. Csöllei, D. Vullo, V. Garaj, P. Pazdera, C.T. Supuran, Novel sulfonamide incorporating piperazine, aminoalcohol and 1,3,5-triazine structural motifs with carbonic anhydrase I, II and IX inhibitory action, Bioorg. Chem., 77 (2018) 25-37.

[19] J.M. Gerdes, D.B. Bolstad, M.R. Braden, A.W. DBarany, 1-[(2'substituted)piperazin-1'-yl)isoquinolines as norepinephrine transporter inhibitor therapeutics and positron emission tomography imaging agents. WO2008115593.

[20] L. Huang, R.J. Kerns, Diversity-oriented chemical modification of heparin: Identification of charge-reduced N-acyl heparin derivatives having increased selectivity for heparin-binding proteins, Bioorg. Med. Chem., 14 (2006) 2300-2313.

[21] K.T. Chapman, K. Dinnell, J.M. Elliott, G.J. Hollingworth, S.M. Hutchins, D.E. Shaw, C.A. Willoughby, 2-aryl indole derivative as antagonists of tachykinins. US6518273 (B1), in, 2003.

[22] D.E. Levy, M.S. Smyth, R.M. Scarbotough, Piperazine and homopiperazine compounds. US2003153556.

[23] A. Jain, S.G. Huang, G.M. Whitesides, Lack of Effect of the Length of Oligoglycine- and Oligo(ethylene glycol)-Derived para-Substituents on the Affinity of Benzenesulfonamides for Carbonic Anhydrase II in Solution, J. Am. Chem. Soc., 116 (1994) 5057-5062.

[24] L. Guandalini, M.V. Martino, L. Di Cesare Mannelli, G. Bartolucci, F. Melani, R. Malik, S. Dei, E. Floriddia, D. Manetti, F. Orlandi, E. Teodori, C. Ghelardini, M.N. Romanelli, Substituted

piperazines as nootropic agents: 2- or 3-phenyl derivatives structurally related to the cognition-enhancer DM235, Bioorg. Med. Chem. Lett., 25 (2015) 1700-1704.

[25] R.G. Khalifah, The carbon dioxide hydration activity of carbonic anhydrase. I. Stop-flow kinetic studies on the native human isoenzymes B and C., J. Biol. Chem., 246 (1971) 2561-2573.

[26] J. Zhang, H. Tsoi, X. Li, H. Wang, J. Gao, K. Wang, M.Y. Go, S.C. Ng, F.K. Chan, J.J. Sung, J. Yu, *Carbonic anhydrase IV* inhibits colon cancer development by inhibiting the Wnt signalling pathway through targeting the WTAP–WT1–TBL1 axis, Gut, 65 (2016) 1482-1493.

[27] H. Barker, M. Aaltonen, P. Pan, M. Vähätupa, P. Kaipiainen, U. May, S. Prince, H. Uusitalo-Järvinen, A. Waheed, S. Pastoreková, W.S. Sly, S. Parkkila, T.A.H. Järvinen, Role of carbonic anhydrases in skin wound healing, Exp. Mol. Med., 49 (2017) e334.

[28] V. Alterio, A. Di Fiore, K. D'Ambrosio, C.T. Supuran, G. De Simone, Multiple Binding Modes of Inhibitors to Carbonic Anhydrases: How to Design Specific Drugs Targeting 15 Different Isoforms?, Chem. Rev., 112 (2012) 4421-4468.

[29] C.T. Supuran, How many carbonic anhydrase inhibition mechanisms exist?, J. Enzyme Inhib. Med. Chem., 31 (2016) 345-360.

[30] T. Stams, S.K. Nair, T. Okuyama, A. Waheed, W.S. Sly, D.W. Christianson, Crystal structure of the secretory form of membrane-associated human carbonic anhydrase IV at 2.8-Å resolution, Proc. Natl Acad. Sci. USA, 93 (1996) 13589-13594.

[31] A.G. Marshall, C.L. Hendrickson, High-Resolution Mass Spectrometers, Ann. Rev. Anal. Chem. , 1 (2008) 579-599.

[32] V. Menchise, G. De Simone, V. Alterio, A. Di Fiore, C. Pedone, A. Scozzafava, C.T. Supuran, Carbonic Anhydrase Inhibitors: Stacking with Phe131 Determines Active Site Binding Region of Inhibitors As Exemplified by the X-ray Crystal Structure of a Membrane-Impermeant Antitumor Sulfonamide Complexed with Isozyme II, J. Med. Chem., 48 (2005) 5721-5727.

[33] C.T. Supuran, F. Mincione, A. Scozzafava, F. Briganti, G. Mincione, M.A. Ilies, Carbonic anhydrase inhibitors — Part 52. Metal complexes of heterocyclic sulfonamides: A new class of

strong topical intraocular pressure-lowering agents in rabbits, Eur. J. Med. Chem., 33 (1998) 247-254.

[34] V. Garaj, L. Puccetti, G. Fasolis, J.-Y. Winum, J.-L. Montero, A. Scozzafava, D. Vullo, A. Innocenti, C.T. Supuran, Carbonic anhydrase inhibitors: Novel sulfonamides incorporating 1,3,5-triazine moieties as inhibitors of the cytosolic and tumour-associated carbonic anhydrase isozymes I, II and IX, Bioorg. Med. Chem. Lett., 15 (2005) 3102-3108.

[35] M. Şentürk, İ. Gülçin, Ş. Beydemir, Ö.İ. Küfrevioğlu, C.T. Supuran, In Vitro Inhibition of Human Carbonic Anhydrase I and II Isozymes with Natural Phenolic Compounds, Chem. Biol. Drug Design, 77 (2011) 494-499.

[36] F. Fabrizi, F. Mincione, T. Somma, G. Scozzafava, F. Galassi, E. Masini, F. Impagnatiello, C.T. Supuran, A new approach to antiglaucoma drugs: carbonic anhydrase inhibitors with or without NO donating moieties. Mechanism of action and preliminary pharmacology, J. Enzyme Inhib. Med. Chem., 27 (2012) 138-147.

[37] A.G.W. Leslie, H.R. Powell, Processing diffraction data with mosflm, in: R.J. Read, J.L. Sussman (Eds.) Evolving Methods for Macromolecular Crystallography: The Structural Path to the Understanding of the Mechanismof Action of CBRN Agents, Springer Netherlands, Dordrecht, 2007, pp. 41-51.

[38] G.N. Murshudov, A.A. Vagin, E.J. Dodson, Refinement of Macromolecular Structures by the Maximum-Likelihood Method, Acta Cryst. Section D, 53 (1997) 240-255.

[39] A.A. Lebedev, P. Young, M.N. Isupov, O.V. Moroz, A.A. Vagin, G.N. Murshudov, JLigand: a graphical tool for the CCP4 template-restraint library, Acta Cryst. Section D, 68 (2012) 431-440.

[40] P. Emsley, B. Lohkamp, W.G. Scott, K. Cowtan, Features and development of Coot, Acta Cryst. Section D, 66 (2010) 486-501.

[41] V.S. Lamzin, A. Perrakis, K.S. Wilson, The ARP/wARP suite for automated construction and refinement of protein models, in: M.G. Rossmann, E. Arnold (Eds.) Int. Tables for Crystallography.

Vol. F: Crystallography of biological macromolecules, Kluwer Academic Publishers, Dordrecht, The Netherlands,, 2001, pp. 720-722.

[42] S.C. Lovell, I.W. Davis, W.B. Arendall, P.I.W. de Bakker, J.M. Word, M.G. Prisant, J.S. Richardson, D.C. Richardson, Structure validation by Cα geometry: ϕ,ψ and Cβ deviation, Proteins, 50 (2003) 437-450.

[43] E.F. Pettersen, T.D. Goddard, C.C. Huang, G.S. Couch, D.M. Greenblatt, E.C. Meng, T.E. Ferrin, UCSF Chimera—A visualization system for exploratory research and analysis, J. Comput. Chem., 25 (2004) 1605-1612.

[44] A. Nocentini, M. Ferraroni, F. Carta, M. Ceruso, P. Gratteri, C. Lanzi, E. Masini, C.T. Supuran, Benzenesulfonamides Incorporating Flexible Triazole Moieties Are Highly Effective Carbonic Anhydrase Inhibitors: Synthesis and Kinetic, Crystallographic, Computational, and Intraocular Pressure Lowering Investigations, J. Med. Chem., 59 (2016) 10692-10704.

[45] Schrödinger, Schrödinger Suite Release 2016-1, Schrödinger, LLC, New York, NY, 2016: (a) Maestro v.10.5; (b) Epik, v.3.5; (c) Macromodel v.11.1.; (d) Glide, v.7.0. (e) Prime, v.4.3.

[46] J. Li, R. Abel, K. Zhu, Y. Cao, S. Zhao, R.A. Friesner, The VSGB2.0 model: a next generation energy model for high resolution protein structure modeling, Proteins 79 (2011) 2794-2812.

[47] K.R. Wilhelmus, The Draize eye test, Surv. Ophthalmol., 45 (2001) 493-515.

[48] F. Galassi, E. Masini, B. Giambene, F. Fabrizi, C. Uliva, M. Bolla, E. Ongini, A topical nitric oxide-releasing dexamethasone derivative: effects on intraocular pressure and ocular haemodynamics in a rabbit glaucoma model, Br. J. Ophthalmol., 90 (2006) 1414-1419.